

**MODEL-BASED FRAMEWORK FOR ALLOY
ELECTRODEPOSITION PROCESSES**

A Thesis

Submitted to the Graduate Faculty of the
Louisiana State University and
Agricultural and Mechanical College
in partial fulfillment of the
requirements for the degree of
Master of Science in Chemical Engineering

In

The Department of Chemical Engineering

by
Miguel E. Estrada
B.S., University of Tulsa, 2005
May, 2008

ACKNOWLEDGEMENTS

I would like to thank Dr. Jose Romagnoli for his advice, support and guidance as well as Dr. Elizabeth Podlaha for her stimulating discussions and valuable input. Dr. Romagnoli has been a great mentor, and a friend to me.

I would like to thank Dr. John Flake and Dr. Francisco R. Hung for accepting to be part of my graduate committee. I would like to acknowledge my colleagues in the Chemical Engineering department, specially my research mates: Rob, Daira, David, Rajib, Ombretta and Swathi for helpful research discussions and friendship and Dr. Pablo Rolandi for his help and advice.

Thanks to my family who has always been a good example of dedication, strength, determination and love. I want to thank my entire family deep inside in my heart for trusting me and being always sure of my success, and Gisela who always believed in me.

This work was supported by the Chemical Engineering Department at LSU.

TABLE OF CONTENTS

ACKNOWLEDGEMENTS	ii
LIST OF TABLES	v
LIST OF FIGURES	vi
ABSTRACT.....	viii
CHAPTER 1 INTRODUCTION	1
1.1 Introduction.....	1
1.2 Goal of Study	4
1.3 Structure of the Thesis	6
CHAPTER 2 ELECTRODEPOSITION SYSTEMS AND MODEL DEVELOPMENT	8
2.1 Electrodeposition Applications and Importance.....	8
2.2 Basic Concepts and Definitions of Electrodeposition Systems	9
2.3 Experimental Setup.....	12
2.4 Mathematical Electrodeposition Models	13
2.4.1 Boundary Layer for Rotating Cylinder and Disk Electrode	14
2.4.2 Treatment of Mechanisms.....	14
2.4.3 Mass Balance Coupled Ordinary Differential Equations.....	17
CHAPTER 3 MODEL IMPLEMENTATION	20
3.1 Introduction to Advanced Equation Oriented Modeling	20
3.2 gPROMS Implementation Introduction.....	22
3.2.1 Algebraic and Ordinary Differential Equations Solvers.....	24
3.3 Non General Model Kinetic Parameters	26
3.4 Interface Implementation	28
3.4.2 Implementation of Front End Application.....	28
3.4.3 Application and Functionality.....	29
3.4.4 Goals and Importance	29
CHAPTER 4 PARAMETER ESTIMATION.....	33
4.1 Introduction.....	33
4.2 Parameter Estimation Mathematical Formulation	34
4.3 Objective Function Maximum Likelihood Estimator	35
4.4 Parameter Estimation Execution Solver	36
4.5 Estimation of Optimal Kinetic Parameter Strategy	37
4.6 Parameter Estimation Study for Single Metal and Alloy Deposition	38
4.7 Capabilities of the Electrodeposition Model.....	46
4.8 Confidence Regions and Statistical Results.....	51
CHAPTER 5 OPTIMIZATION STUDIES	54
5.1 Introduction.....	54
5.2 Optimization Overview: Objective Function.....	55

5.2.1 Point and Dynamic Optimization in gPROMS	57
5.3 Practical Applications	58
5.3.1 Optimization Execution	60
5.4 Optimization Studies Conclusion	65
CHAPTER 6 CONCLUSIONS	66
REFERENCES	69
VITA	72

LIST OF TABLES

Table 2-1: Reduction reactions in NiCoFe and NiCoFeCu/Cu systems.....	15
Table 2-2: Tafel approximations.....	16
Table 3-3: Zhuang’s kinetic estimated parameters	27
Table 4-1: Kinetic parameters estimated using various electrolyte compositions for single and alloy depositions	38
Table 4-2: Parameter estimation specifications and results for single metal deposition	39
Table 4-3: Parameter estimation specifications and results for alloy deposition.....	44
Table 5-1: Point optimization problem 1 results.....	61
Table 5-2: Dynamic optimization problem 2 part a results	62
Table 5-3: Dynamic optimization problem 2 part b results	63
Table 5-4: gPROMS schedule sequence for the process entity	64

LIST OF FIGURES

Figure 2-1: Schematic of a basic electrochemical cell.....	10
Figure 2-2: Polarization curve for codeposition systems.....	12
Figure 2-3: Flow profile for a rotating disk electrode.....	18
Figure 3-1: Equation comparisons from paper to gPROMS language	21
Figure 3-2: Model entity partitioned simplified sections.....	23
Figure 3-3: Process entity partitioned simplified sections.....	23
Figure 3-4: Front end interface implementation.	30
Figure 3-5: Executed front end interface implementation	31
Figure 4-1: Simulated (a) Co (b) Fe (c) Ni (d) Cu single metal deposition partial current density using optimal kinetic parameters	41
Figure 4-2: Simulated (a) Co and (b) Fe partial current density during alloy metal deposition using optimal kinetic parameter estimates	45
Figure 4-3: Simulated side reaction partial current density during alloy metal deposition using optimal kinetic parameter estimates.....	46
Figure 4-4: Enhancement effect simulation for iron partial current at a concentration of single metal deposition of (a) 0.05M (b) 0.1M and ternary alloy deposition.....	47
Figure 4-5: Inhibition effect simulation for nickel partial current density at a concentration of single metal deposition of 0.2M and ternary alloy deposition with changes in iron concentration of (a) alloy Fe(0.025M) (b) alloy Fe(0.08M).	48
Figure 4-6: Surface coverage simulation by iron species during ternary alloy deposition of Ni(0.2M)Co(0.1M)Fe(0.025M).	50
Figure 4-7: Influence of iron bulk concentration on the partial current density of nickel.....	50
Figure 4-8: Confidence ellipsoid for Tafel slope and rate constant of Ni for reaction one	52
Figure 4-9: Confidence ellipsoid for Tafel slope and rate constant of Ni for reaction two.....	52
Figure 4-10: Confidence ellipsoid for Tafel slopes of Ni reactions.....	53

Figure 5-1: Example of a fixed concentration of electrolyte, composition vs. potential (V)61

Figure 5-2: Metal compositions vs. thickness (nm)65

ABSTRACT

The electrodeposition of iron-group alloys has been widely studied due to their interest as materials used for their magnetic and thermo-physical properties. Models such as ternary NiCoFe and quaternary NiCoFeCu multilayer alloys have been previously developed to simulate mass transfer and reaction kinetics. The reactions involved in the models contain kinetic parameters such as rate constants and inverse Tafel slopes which are estimated using trial and error techniques. The previous models are limited to a set of kinetic parameters for each change in concentrations of the electrolyte. Although deposition behaviors such as anomalous codeposition are captured, functionalities to use the models as a tool for interesting deposition schemes are not possible without a single set of kinetic parameters. Therefore, in this project, the use of advanced modeling approaches is investigated to capture the influence of key operating variables affecting the process.

Parameter estimation, based on the maximum likelihood theory, is defined and tested successfully to estimate all kinetic parameters for a wide range of concentrations. The general set of kinetic parameters is fully validated against experimental data and statistical analysis tools are used to evaluate confidence regions. The modeling work is carried out using the gPROMS open modeling software which provides a complete environment for modeling complex systems. All phases of model development are supported by gPROMS which offers a selection of techniques for solving specific problems. Using the open modeling capabilities, the model is developed into a front end application using VBA in excel. This application allows the model to be used by non expert programming users to evaluate electrodeposition behaviors and key variables which play a role into fabricating novel deposition materials. Subsequent to the validation step, the model is used within an optimization framework towards the development of a general method for reproducible production electrodeposition schemes of nanometric multilayers. Successful results

are obtained for finding the concentrations and potential needed to deposit fixed compositions of the alloy. Dynamic optimization is tested to develop a time schedule (optimal deposition scheme) aiming at the deposition of a fixed thickness for each multilayer deposition of NiCoFe alloy with Cu.

CHAPTER 1. INTRODUCTION

This chapter serves as an introduction to advanced equation oriented modeling focusing on electrodeposition processes. Specifically two systems are selected for the study: a steady state ternary NiCoFe alloy deposition and a dynamic quaternary multilayer NiCoFeCu/Cu alloy deposition. The desired properties and importance of iron group alloys such as nickel, cobalt and copper will be reviewed. The motivations of electrodeposition process modeling, as well as objectives and goals, which include a systematic approach to electrodeposition modeling to include simulation, parameter estimation and optimization environment, are shown. The last part of the chapter will provide a summary of how objectives are to be accomplished as well as an introduction to the structure of the thesis.

1.1 Introduction

Electrodeposition refers to a process by which an applied current or potential is used to deposit a film of single or alloy metal to a conductive substrate by reduction of metallic ions from an electrolyte solution. Extensive studies have been performed on metal depositions, where primary application is to deposit layers that have desired properties. Iron group alloys research studies have focused on magnetic properties such as electrical resistivity, magnetoresistance and other properties such as corrosion resistance which depends on the deposit composition and microstructures which are controlled by solution composition and deposition variables. Electrodeposited iron group alloys such as nickel, cobalt and iron are of interest for their unique magnetic and thermo-physical properties¹⁻³. They have been used for recording, memory, storage devices and other applications⁴⁻⁸. These alloys layered with copper at the nanoscale⁹⁻¹⁰ have been found to exhibit giant magnetoresistance (GMR), a change in the materials resistance with an applied magnetic field, used as a sensor material to retrieve magnetic data¹¹⁻¹².

Most work reported on parameters affecting the electrodeposition of iron group alloys, consist of extensive empirical work. Complex mechanisms of alloys have been studied, where mathematical deposition models have been developed and range from single depositions to alloys. Such models have been developed on binary systems. Matlosz¹³ developed a competitive adsorption model to study nickel and iron codeposition, by combining two step reaction mechanisms. Hassami and Tobias¹⁴ developed a mathematical model for anomalous codeposition of nickel-iron, which predicted features of anomalous codeposition. Sasaki and Talbot¹⁵⁻¹⁶ developed a supportive model of iron-group electrodeposition. The models mentioned are binary systems where Podlaha's group¹⁷⁻¹⁸ has expanded to tertiary and quaternary systems where as the system becomes more complex, the number of parameters to measure and estimate increases significantly. Zhuang and Podlaha have developed a steady state mathematical model to simulate the mass transfer and reaction kinetics involved for the NiCoFe alloy depositions¹⁻³. Huang and Podlaha¹⁷⁻¹⁸ have expanded Zhuang's model to a non steady state multilayer quaternary system of NiCoFeCu/Cu.

Mechanisms of the alloy deposition provide insight of anomalous deposition behavior which refers to preferential deposition of the less noble metal¹⁹. The coupled reaction kinetics has been described by an adsorption approach. The less noble metal preferentially adsorbs onto the electrode surface and blocks the codeposition of the other iron-group elements, Co and Ni. In certain cases the less noble metal can also be accelerated and has been modeled by treating the more noble species as a catalyst²⁰. Both features have been combined by Zhuang and Podlaha¹⁻³ as well as Huang and Podlaha¹⁷⁻¹⁸ to predict a combined apparent inhibition and acceleration effect of the codeposition system. Since the reaction kinetics are dependent upon concentration, mass transport also plays a role when the driving force (i.e. applied potential or applied current)

is large. Both models rely on trial and error procedure in order to estimate kinetic parameters and fit them to experimental data.

The optimization of kinetic parameters in electrodeposition models is an important issue to produce a quality model. Parameter estimation is critical in order to improve the accuracy of the model for the model predictions, to match measured data and simulated values. Previous model estimations performed for ternary and quaternary electrodeposition systems are often ambiguous due to subjective, trial and error attempts to match observation and predictions. The trial and error process is a very tedious and time consuming task, depending on the number of correlated parameters, which increase as more reactions are added to a system. Not many mathematical estimation algorithms have been attempted in electrodeposition models. An important and popular parameter estimation technique is the maximum likelihood estimator. Maximum likelihood is a mathematical optimization technique that attempts to find a “best fit” to a set of data by maximizing the likelihood of predicting the experimental set of measurements (or minimizing the error between the experimental measurements and predicted values instead)²¹. The method of maximum likelihood estimation is considered to be robust, and yield estimates with good statistical properties, which have been proven in many models and types of data for various applications²².

Equation oriented modeling language approaches have evolved into multi-purpose process-engineering software tools which can be used in activities such as steady state and dynamic simulations, steady state and dynamic optimization, parameter estimation and mixed integer/dynamic optimization. Rolandi and Romagnoli²³⁻²⁵ have recently proposed a novel model-centric framework for integrated simulation estimation/reconciliation and optimization of systems based on mechanistic process models. These model based frameworks are used to develop accurate predictive models that are used for different activities in analyzing, and

optimizing a wide range of processes to improve design solutions and provide high level equation oriented modeling languages.

A true process modeling tool which is not restricted to just a simulator can represent using a set of equations chemical and physical relationships within equipment and their operation procedures. Advantages such as open architecture helps in linking software to any external software running on any platform, allowing tailored solutions to be built from a wide variety of components. Most software available today hides from the user the underlying mathematical complexity, to focus on simulation results, and understanding of the topics. Graphical user interface designs can be developed to enhance the usability of complex programs to non programming users.

1.2 Goal of Study

The goal of this study is to propose a systematic approach to electrodeposition systems, in which using equation based modeling a novel model centric framework for integrated simulation, estimation and optimization can be implemented. The framework will not be limited to just simulation. Kinetic parameters such as rate constants and Tafel slopes which as mentioned before were previously estimated using trial and error procedures will be optimized using the parameter estimation entity. Previous mathematical models such as ternary system by Zhuang and Podlaha¹⁻³ contain a set of parameters for different concentrations of the alloys, where for example if the concentration of a simulation is changed, then different kinetic parameters for the reactions are used. Using parameter estimation techniques where all experimental data for a range of concentrations can be used will provide a general model, with only one set of kinetic parameters. The general model can then be used to test various concentrations and interesting deposition schemes. Once a general model is found with parameter estimation techniques then the optimization entity to maximize or minimize an objective function, can be used with

constraints, to study composition, thickness and other useful results to later implement in an experimental run. Included in the thesis goals, is the development of a graphical user interface developed in Excel with visual basic programming to be able to study electrodeposition systems, which will give value to the model to be used by non modeling users to provide model based decision support, and easy deployment of models, as well as an easy transfer of the electrodeposition models between users.

gPROMS leading advanced process modeling environments will be used for our approach. Taking advantage of the functionalities of the capabilities of modern modeling the first step will be to implement the ternary steady state model and then expand to a quaternary multilayer dynamic model into gPROMS modeling language. Analysis of the robust solvers will be studied in order to represent previous simulation results. Once the model is completely defined the next step is to include parameter estimation studies for kinetic constants which include Tafel slopes and rate constants. A maximum likelihood estimation technique will be tested for these parameters used in current density equations. Estimated parameters will be used and fitted to experimental data of various concentrations, in hopes of creating a general model. A validation step with different sets of data will be undertaken as well as a statistical validation theory. Statistical analysis from parameter estimations can be taken into consideration in order to provide a sensitivity analysis to evaluate features of the model that are most important and sensitive to the operating conditions. The final validated model can be used for manufacturing of interesting deposition schemes. Apart from estimation of parameters, the optimization entity will be tested to solve interesting problems where an objective function will be maximized or minimized, taking into account constraints and a control variable. Several problems will be presented to test the capabilities of optimization, both for point optimization in the case of the ternary system and dynamic optimization for the quaternary system. The last part of the research

will consist in providing versatility and ease of use to electrodeposition models in which a front end application will be developed using Excel and Visual Basic. Features of the front end will provide ease of use to non programming expert user to run simulations and estimations and compare it directly with experimental data. By encapsulating the complex interactions at the interface level within a mechanistic model, describing the compositional gradients of each magnetic layer, the formulation of a model-centric strategy to support the experimental investigations will result in our approach.

1.3 Structure of the Thesis

The structure of the thesis consists of seven chapters. A summary of each is given below except for chapter one which is the introduction chapter.

Chapter two reviews the basic concepts and definitions of electrochemical systems as well as model development. Starting with the importance and application in electrodeposition processes and focusing on two systems, a ternary NiCoFe alloy deposition, and an expanded quaternary multilayer NiCoFeCu/Cu alloy deposition. Experimental design procedures and electrolyte concentrations for each deposition using rotating disk electrode and rotating cylinder electrode deposition schemes are discussed. This chapter also introduces the mathematical model equations which simulate the mass transfer and reaction kinetics involved in alloy deposition used for our approach. Both steady state ternary and non-steady state quaternary systems model equations are discussed.

In Chapter three, an introduction to equation oriented modeling is given leading into the description of gPROMS entities and procedures to implement the mathematical model equations. Solvers used for differential and algebraic equations for simulations, optimization and parameter estimation are defined. gO:Run license and foreign object implementation are discussed Finally,

the interface implementation and explanation is illustrated, where some general simulation results are shown to emphasize on the advantages of the front end application.

Chapter four will focus on formulating and testing the maximum likelihood estimator, to find the best fit for our experimental data consisting of partial current densities at different concentrations of the alloy. The parameters which to be estimated will consist on the kinetic parameters used in Tafel approximations of the current densities and statistical analysis tools are discussed to define confidence intervals for the estimated parameters. Using the optimal parameters, simulation results for current densities will be validated and tested against experimental data. The capabilities of the electrodeposition models will be shown by simulating several cases where anomalous codeposition behaviors such as inhibition and enhancement effects are present.

In Chapter five the dynamic and point optimization entities to be included in the framework will be discussed. The capabilities of solving difficult problems using optimization techniques by maximizing or minimizing a given objective function using certain control variables and constraints will be shown. Several detailed problems are illustrated with detailed optimization procedures and results.

Finally, the main conclusions from this research are included in Chapter 6, where a number of recommendations are also suggested for future studies.

CHAPTER 2. ELECTRODEPOSITION SYSTEM AND MODEL DEVELOPMENT

The electrochemical mathematical equation description for the ternary NiCoFe and multilayer NiCoFeCu/Cu alloys will be the main focus of this chapter. Model equations described can be used to simulate mass transfer and reaction kinetics involved in alloy deposition. A brief introduction of electrochemical systems will be given as well as experimental setup used for the two systems consisting of rotating disk and cylinder electrodes. The experimental data from the experiments provide the model data to later advance into parameter estimation.

2.1 Electrodeposition Applications and Importance

Electrodeposition is an important and widely used technology, which versatility allows the tailoring of surface properties of a bulk material by varying the composition and structure. Produced deposits meet a variety of demands of the researchers and designers. Electrodeposition is economically efficient and applicable to irregular geometries which attract various applications. The primary application is to deposit films of single metal or alloys with a desired property onto a conductive substrate surface which does not contain the property of interest. The unit operations are complex because of the large number of critical elementary process steps to control the overall process. Many scientific disciplines contribute to the topic some include surface science, solid state physics, metallurgy and material science, electronics, electrochemistry and electrochemical engineering. Electrodeposited materials, for various applications include both physical and mechanical material properties. Physical properties consist of electrical and thermal conductivity, magnetic behavior, thermoelectric effects, density, melting point, lattice structure and others²⁶. Mechanical properties have to do with elastic modulus, hardness, ductility and strength. Various factors affect deposition coatings where extensive electrochemistry empirical work is available.

Electrodeposition in fabrication technology is growing and very important in microelectronics industry. A wide range of technological areas use electrodeposition methods. Applications include contacts, connectors, magnetic recording heads, for optics, opto-electronics, sensors and others. Microdevices structure which range from thin to thick three dimensional structures containing properties such as corrosion protection, abrasion resistance and wear, thermal, magnetic are possible through electrodeposition.

The electrodeposition of iron-group alloys has been widely studied due to their interest as materials used in computer magnetic data storage and sensing²⁷⁻²⁹. Depositions of nickel and iron binary alloys have been found to be useful for recording, memory and storage devices⁴⁻⁸. Nickel, cobalt and iron ternary alloys which thin magnetic heads have been used for high density recordings because of a high magnetic flux density and lower coercivity than Permalloy(Ni80Fe20)³⁰. Nanometric multilayers alloys consisting of Nickel, iron and cobalt layered with copper have received attention for exhibiting giant magnetoresistance. Other applications include laser housings, microwave guides and printed wired boards and micro-electro-mechanical systems technology³¹⁻³².

2.2 Basic Concepts and Definitions of Electrodeposition Systems

Electrodeposition also called electroplating refers to a process by which an applied current or potential is used to deposit a coating of single or alloy metal to a conductive substrate by reduction of metallic ions from an electrolyte solution. An electrolytic cell is used which contains the anode and cathode connected to an external supply of direct current. The cathode which is the object to be plated is connected to the negative terminal, and the anode to the positive terminal of the supply. The anode can be the metal being deposited in single depositions or an inert material such as platinum where the anodic reaction is oxygen evolution. An electrolyte bath contains the salt of metal(s) to be deposited, the metallic ions of the salt which

carry a positive charge are attracted to the cathode and the supplied electrons reduce the positively charged ions to metallic zero valence state. The reference electrode is used as a reference point against which the potential of the working electrode can be measured. A schematic of a basic electrochemical cell is shown in Figure 2-1.

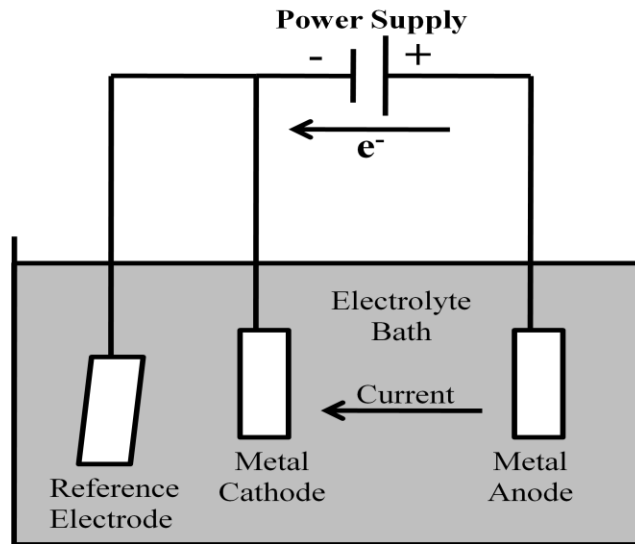


Figure 2-1: Schematic of a basic electrochemical cell

Elementary reduction reactions of the metal ions from salt electrolytes usually involve one electron transfer. For a deposition mechanism the overall form of the reaction that occurs in the aqueous medium at the cathode is



The deposition reaction current density which units correspond to amperage of the electrodeposition current divided by the surface area of the cathode electrode will depend on the electrolyte concentration of the metals and applied potential and can be quantified by kinetic Tafel expressions as follows.

$$\frac{i}{nF} = k(C_{M^{n+}})^{p_m} \cdot \exp\left(\frac{-b_k \eta}{RT}\right) \quad [2.2]$$

Where i is the reduction current density, n is the number of electrons transferred, F is Faraday's constant, k the rate constant $C_{M^{n+}}$ the surface concentration of the metal, b_k the inverse Tafel slope and η the difference between the applied potential E and the equilibrium potential E_{rev} . From equation 2.2 the relation between current and applied potential is found. The inverse Tafel slope depends of temperature as follows and has units of $1/V$

$$b_k = \frac{\alpha F}{RT} \quad [2.3]$$

Where α is a transfer coefficient for the cathodic reaction.

Figure 2-2 shows a polarization behavior for an ideal alloy codeposition system of two metals. At low applied potential there is kinetic control, since the bulk concentration of the metal ions equals the surface concentration. At higher applied potentials a gradient of ions develops at the electrode surface when surface concentration becomes less than bulk concentration mass transport becomes dominant. For the ideal system the deposition current of alloy M_1 and M_2 is the sum of the single metal partial current. Nernst equilibrium potential for each metal dictates which metal deposits. The more noble element, (1), the one with the largest equilibrium potential, is first favored to deposit, followed by the less noble (2). M_1 deposits first at low applied current or more noble potentials. When the potential becomes more negative, or as the applied current increases, M_2 codeposition begins, and an alloy deposits. Potential versus current plots are effective tools to provide information necessary to select an appropriate potential for the reduction of desired metals, where interesting multilayer depositions can be obtained such as NiCoFeCu/Cu, where the copper layers are deposited at low potentials, and the alloy at higher potentials.

The Tafel behavior is found when the partial current of the metals rise exponentially as the electrode potential moves negative of the equilibrium potential. It is important to determine

the information necessary to select the accurate potential for the reduction of desired metals. The ratio of the amount of each metal deposited in alloys will depend strongly on the relative concentrations of the solution, but are not necessarily proportional due to the coupled nature of the kinetics.

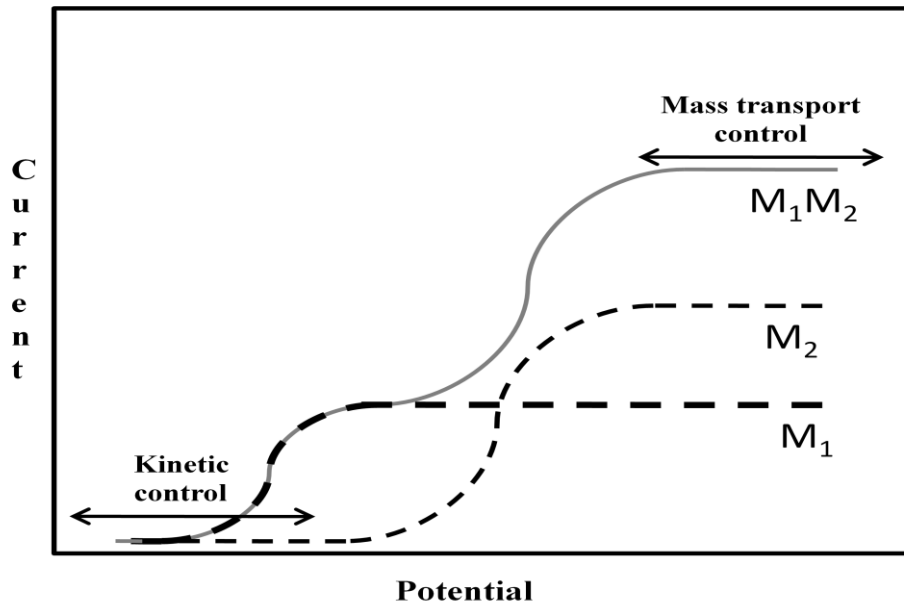


Figure 2-2: Polarization curve for codeposition systems.

There are many factors that influence the composition and morphology of electrodeposition. Most empirical studies cite the influence of various factors on the electrodeposition of alloys, such as electrolyte concentrations, temperature, pH, complexing agents and current densities. The model presented here will address all of these except complexing agent affects.

2.3 Experimental Setup

Various experimental procedures have been developed for electrodeposition research studies. The two models used for the study, were developed using experimental observations in order to match simulation results. Ternary deposition experiment data of NiCoFe was found using a hydrodynamic rotating cylinder electrode system (RCE) and the quaternary system

experimental data NiCoFeCu/Cu using a rotating disk electrode system (RDE). The electrodes are rotated at a constant frequency in solution. A summary of the experimental setup performed by Zhuang¹⁻³ and Q.Huang¹⁵⁻¹⁶ and experimental data will be presented. The rotating systems were used so that mass transfer boundary layer sizes could be easily controlled and reproducible. The RCE results in turbulent flow near the electrode surface, while the RDE creates a laminar flow environment at the electrode.

Galvanostatic deposition is carried out for both systems using a BAS-Zahner IM6(e) system with a PC and an impedance measurement unit to control de current. The mass of the electrodes are measured before and after the deposition using a Mettler AE 240 and AE 50 balances. The deposition chemical composition is analyzed by a Superprobe 733 electron microprobe with a wavelength dispersive X-ray spectrometer, and compared to analysis by a Kevez X-ray fluorescence system. A two compartment cells are used which separate the catholyte and anolyte, where for the anode a piece of platinum mess is used. The reference electrode used is a Corning saturate calomel electrode (SCE). The electrode used for the ternary system is stainless steel, and for the quaternary system a stainless steel, gold plated in order for stripping of the deposit to be performed to calculate for current efficiencies. More detailed experimental setup can be found in Dissertations of Qiang Huang³³ and Yun Zhuang³⁴.

2.4 Mathematical Electrodeposition Models

Two mathematical models which simulate the mass transfer and reaction kinetics involved in alloy depositions will be used. The model from Zhuang and Podlaha¹⁻³ is a steady state ternary alloy deposition of nickel, cobalt and iron. The second model from Huang and Podlaha¹⁷⁻¹⁸ expands to a quaternary multilayer system of nickel, cobalt, iron and copper at steady and non steady state behavior.

The expanded quaternary system which includes copper differs from the ternary system in the calculation of the boundary layer where different electrodes for the deposit are used. The other difference is that for the ternary alloy model, mass transport in the electrolyte consists of diffusion only and in the expanded quaternary system it depends on diffusion and convection only. The rest of the equations are the same, so a combined explanation of the mathematical models will be presented. Model assumptions are included in the model. The Langmuir adsorption assumptions are used, such as uniformly energetic sites, monolayer of coverage and no interactions between adsorbed molecules.

2.4.1 Boundary Layer for Rotating Cylinder and Disk Electrode

For the ternary alloy deposition a rotating cylinder electrode (RCE) is used as the cathode. The boundary layer is determined from the empirical Eisenberg³⁵ equation for rotating cylinder electrodes shown in equation 2.4. For the quaternary multilayer alloy deposition a rotating disk electrode (RDE) is used as the cathode. The boundary layer thickness is determined from the empirical Levich³⁶ equation for rotating disk electrodes shown in equation 2.5.

$$\delta_{\text{RCE}} = 99.62^{-0.4} \nu^{0.344} D^{0.356} S^{-0.7} \quad [2.4]$$

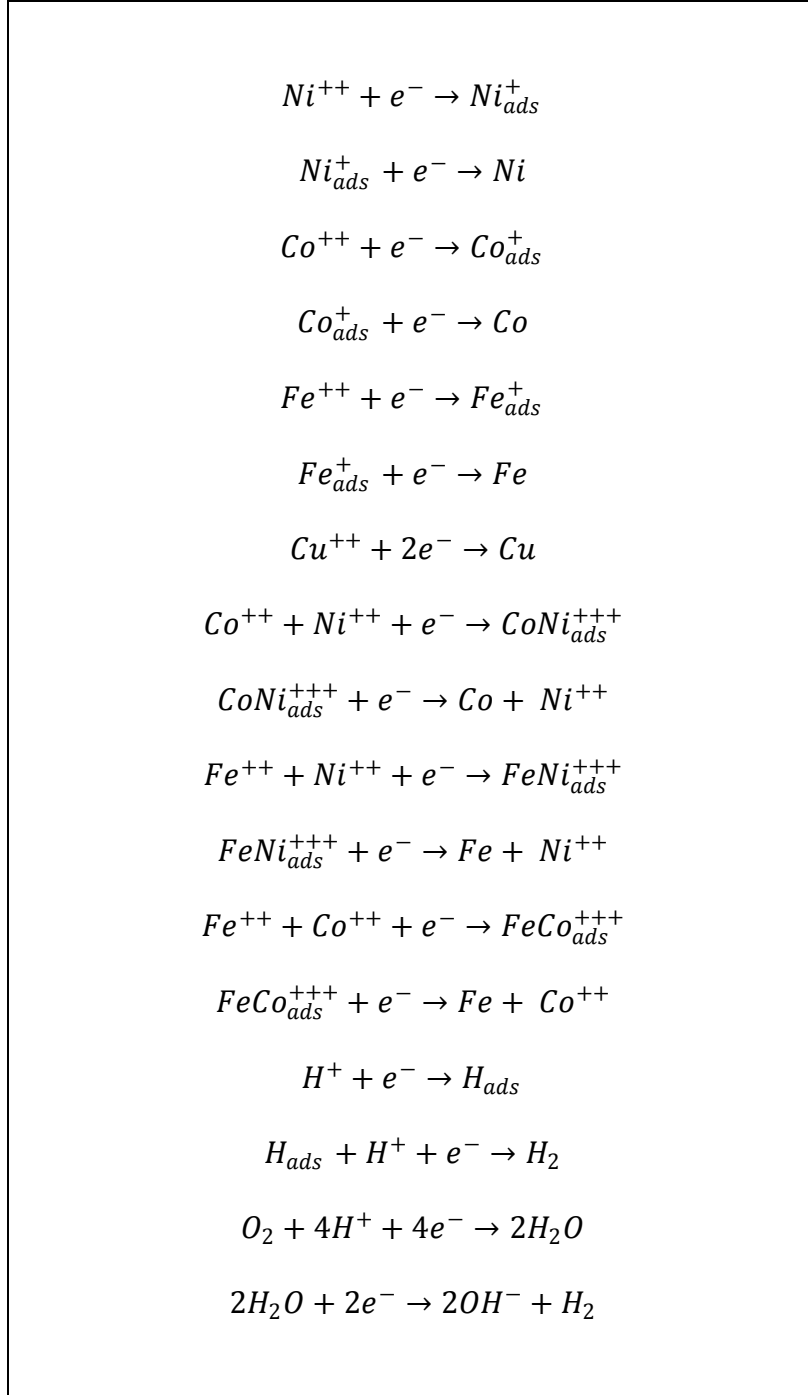
$$\delta_{\text{RDE}} = 1.61 \cdot D^{1/3} \cdot \omega^{-1/2} \cdot \nu^{1/6} \quad [2.5]$$

Where, D is the diffusion coefficient, ν the kinematic viscosity ω the angular velocity and S the rotation rate. The boundary is used in diffusion equations to relate concentration to distance x from the electrode surface. It is used as the axial coordinate distance for the model simulation.

2.4.2 Treatment of Mechanisms

Reduction reactions for NiCoFe ternary alloy deposition are shown in Table 3.1 as well as the copper reaction added for quaternary NiCoFeCu/Cu system.

Table 2-1: Reduction reactions in NiCoFe and NiCoFeCu/Cu systems



In real electrodeposition systems kinetics of electron transfer between the electro-active species in the electrolyte solution and the electrode will partly determine the net current flowing. Reaction Mechanisms for the metal depositions on the cathode surface are simulated using a two

step manner. Since reactions are controlled by kinetics, then the rate which is described in electrochemistry as the partial current densities (i_{M_j}), is dependent upon potential, E, rate constant, k, species concentrations (mol/cm³) in the electrolyte at the electrode surface C and adsorbed species Θ . The current densities are represented by Tafel expressions for reactants M, and species j in the reaction. Side reactions are also represented by Tafel expressions, where a Volmer-Heyrovsky mechanism is used for the reduction of proton of the hydrogen ion reduction. Reduction of oxygen and the dissociation of water are both accounted for with a simplified one-step reaction. Tafel approximations both for the two step manner and catalytic step for mixed metals are summarized in Table 2-2.

Table 2-2: Tafel approximations

Two step Manner	
$M_j^{++} + e^- \leftrightarrow M_{j,ads}^+$	[2.6]
$i_{M_j} = -F * k_{M_j} * C_{M^{++}} * (1 - \theta) * \exp(-b_{M_j} * E)$	[2.7]
$M_{j,ads}^+ + e^- \leftrightarrow M_j$	[2.8]
$i_{M_j} = -F * k_{M_j} * \theta_{M^+} * \exp(-b_{M_j} * E)$	[2.9]
Catalytic Step for mixed metals.	
$M_1^{++} + M_2^{++} + e^- \leftrightarrow [M_1M_2]_{ads}^{+++}$	[2.10]
$i_{M_1M_2j} = -F * k_{M_1M_2j} * C_{[M_1M_2]^{++}} * (1 - \theta)^2 * \exp(-b_{M_1M_2j} * E)$	[2.11]
$[M_1M_2]_{ads}^{+++} + e^- \leftrightarrow M_1 + M_2^{++}$	[2.12]
$i_{M_1M_2j} = -F * k_{M_1M_2j} * \theta_{[M_1M_2]^{+++}} * \exp(-b_{M_1M_2j} * E)$	[2.13]

The fraction of available surface sites (θ_e) is determined by taking into account the occupied surface coverage of metal ions. Surface coverage is solved assuming simultaneous reactions, where the results are qualitative.

$$\theta_{\text{empty}} = 1 - \sum_j \theta_j \quad [2.14]$$

2.4.3 Mass Balance Coupled Ordinary Differential Equations

Electrochemical transport problems consisting of diffusion and convection are the most challenging to solve, commonly the basic mathematical equations that are solved consist of diffusion equation which relate the concentration to time and distance from the surface of the electrode. In the case of the mass balances for both systems, they differ in that for ternary alloy only diffusion exists, and with the quaternary system both diffusion and convection are modeled. The diffusion flux of each species j at the cathode surface (boundary layer = 0) is related to the electrochemical reaction.

$$D_j \frac{\partial C_j}{\partial x} = - \sum_k \frac{i_k}{n_k F} \quad [2.15]$$

At the cathode and diffusion layer the water dissociation is used

$$K_{H_2O} = C_H^+ * C_{OH^-} \quad [2.16]$$

The material balance of each species in the electrolyte is assumed to be at steady state and is governed by the change of the diffusion flux. A Nernst boundary layer approach is taken for NiCoFe ternary alloy model assuming that there is no convection or migration within the boundary layer.

$$D_j \frac{d^2 C_j}{dx^2} = 0 \quad [2.17]$$

At the end of the diffusion layer the concentration of metal ions equals its bulk concentration. One spatial direction is required for modeling rotating disk and cylinder electrodes. Figure 2.3 shows the flow profile for a rotating disk electrode.

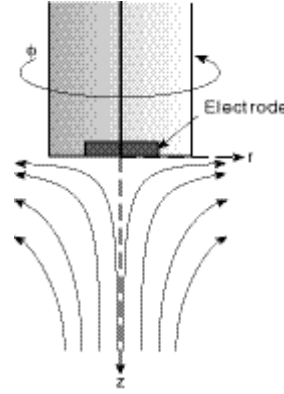


Figure 2-3: Flow profile for a rotating disk electrode³⁷.

Mass transport in the electrolyte consists of diffusion and convection only for quaternary NiCoFeCu/Cu system. The mass balance is governed by

$$\frac{\partial C_j}{\partial t} = D_j \frac{\partial^2 C_j}{\partial x^2} - u_x \frac{\partial C_j}{\partial x} \quad [2.18]$$

Where x and u_x are the axial coordinates from the RDE surface and the axial velocity, respectively. u_x is analytically derived as

$$u_x = -0.51023 \cdot \omega^{3/2} \nu^{-1/2} \cdot x^2 \quad [2.19]$$

u_x used in the convective flux term can be determined analytically for laminar flow, but it is not possible for turbulent flow. In this case, since the diffusional flux is much greater than the convective flux within the diffusion layer, it is neglected within the diffusion layer. The initial and boundary conditions for equation 4.1 are:

$$\text{at } t = 0, x \geq 0 \quad C_j = C_j^{bulk} \quad [2.20]$$

$$\text{at } t > 0, x = \infty \quad C_j = C_j^{bulk} \quad [2.21]$$

$$at t > 0, x = 0 \quad D_j \frac{\partial C_j}{\partial x} = - \sum_k \frac{i_k}{n_k F} \quad [2.22]$$

For those reduction mechanisms with adsorbed intermediates involved, the difference of the rates of the two consecutive steps results in the change of the surface coverage of the associated intermediate.

$$\frac{\partial \theta_j}{\partial t} = -A(i_{j,1} - i_{j,2}) \quad [2.23]$$

Where A is the surface area occupied by a unit amount of the adsorbed intermediates, calculated as $(2.5 \cdot 10^{-16}) N$ Avogadro cm^2/mol . The thickness d, is also determined from current densities and molecular weight of the metals. The weight percent composition of the alloy is determined from the partial current densities and their molecular weight M .

$$d = \sum_{\Delta t} \sum_j \left(\frac{MW_j}{\rho_j} \sum_k \left(\frac{i_k \Delta t}{n_k F} \right) \right) \quad [2.24]$$

As mentioned the model does not take into account formation of different phases, nor nonuniform nucleation.

CHAPTER 3. MODEL IMPLEMENTATION

Implementation using advanced equation oriented modeling of electrodeposition mathematical models will be the main focus of this chapter. The systematic model based framework approach will be tested using gPROMS advanced modeling environment. Previous non general model kinetic parameters will be shown to emphasize on the importance of parameter estimation studies. Foreign object implementation to develop a front end application will be presented as well as solvers for differential and algebraic equations used for simulation, optimization and parameter estimation entities.

3.1 Introduction to Advanced Equation Oriented Modeling

Advanced equation oriented modeling applications have gained increase acceptance versus legacy applications developed by programming languages such as FORTRAN (Formula translation high level language). Many advantages have been found where the objective is to tackle the full scope and detail of process models³⁸. In the case of the electrochemical models of Huang and Podlaha¹⁸ and Zhuang and Podlaha² the FORTRAN language has been used for both alloy models discussed. A change into more advanced environments gives researchers the ability to capture process physics, chemistry and operating conditions in an efficient and successful model form. Independence between mathematical models and solution methods gives the environment a chance to use a single model to complement model based applications.

gPROMS (general process modeling system) advanced modeling capabilities, have been expanded to account for declarations of parameter estimation and optimization activities where model advantages such as reusability and consistency are emphasized. The reuse and transfer of FORTRAN models is difficult for anyone other than the original programmer, because codes can be difficult, where debugging might not be an easy task. Is it important to avoid duplication of modeling efforts for research projects, in which development or upgrades is the focus. The most

limiting part of the simulation implementation written for both electrodeposition systems studied is that the code is written for a specific purpose, where the mathematical equations could be solved only in one direction to generate output values for given inputs. In gPROMS equation oriented modeling, the mathematical complexity is hidden from the user, where the main focus shifts from programming code to actual engineering research task. The mathematical models of complex processes are easily transferred and understood by other users where the procedure to write the equations is similar to how they would appear in a publication. An example to illustrate the advantage over traditional programming codes is shown in figure 3-1. Equation oriented modeling keeps evolving into more concise language editors, where documenting of work can capture the knowledge of the models. These advantages help in model transfers to develop more sophisticated and updated models. The principle of hierarchical sub model decomposition is found in gPROMS language, where complex models can be build from elementary ones.

The figure illustrates the conversion of a mathematical equation from a paper format to gPROMS code. On the left, the equation is presented in a standard mathematical notation:
$$\frac{\partial C_{Fe}}{\partial t} = D_{Fe} \frac{\partial^2 C_{Fe}}{\partial x^2} - u_x \frac{\partial C_{Fe}}{\partial x}$$
 This equation is enclosed in a rounded rectangular box. An arrow points from this box to the right, where the corresponding gPROMS code is shown:
$$C_Fe(z) = D_Fe*PARTIAL(C_Fe(z),Axial, Axial) -ux(z)*PARTIAL(C_Fe(z),Axial)$$

Figure 3-1: Equation comparisons from paper to gPROMS language

Previous electrodeposition models developed in FORTRAN to perform steady state and dynamic simulations would require extensive programming work to include parameter estimation and optimization applications. The most work intensive endeavor consists in developing solution algorithms and using several parts of the original model for the new applications, which is a mayor task for non expert programmers. An environment such as gPROMS which contains models for multiple purposes such as simulation, parameter estimation and optimization give advantages into model reusability and consistency. A single fundamental

process model description which can be used for different model based applications contained by frameworks is beneficial to model developers and expert users. Modeling development strategies and implementation could be distributed into various model based activities, in the case of electrodeposition systems, the estimation of rate constants and inverse Tafel slopes could be performed taking advantage of parameter estimation techniques, for model validation. A range of activities included in the framework, could help in updates and upgrades to the model, where optimization, and experiment design could be used, to test key variables and capabilities. Overall having a single robust model into different model based activities will provide additional benefits and most important a consistency in results.

3.2 gPROMS Implementation Introduction

gPROMS general process modeling software provides an environment which can be used for modeling the behavior of various complex systems, in this case an electrodeposition system, where a combination of processes and equipment models can be found rather than just a narrow view of first generation simulation tools. gPROMS project consists of group of entities which are composed of the following: variable types, stream types, models, tasks, processes, optimizations, estimations, experiments, saved variable sets and Miscellaneous files³⁹⁻⁵⁰.

Each entity is partitioned into a section where required information to define the activity is introduced. A mathematical description of the physical behavior of the system is declared in the Models entity which contains parameters and variables that characterize the system. Description of each entity can be written on the property tabs of each which allows for information that can be used for reference. Variables which are declared need to be specified in the variable types entity in order to provide upper and lower bounds, and initial guesses which are used for initialization. Units of measurements can be introduced, for referencing, which gives facilities in transferring and support of models. Variable types entity are critical since by giving a upper and

lower bound for the variables the execution of the simulation will notify if simulation results are within bounds, to be able to test the model for different operating conditions. Figure 3-2 contains a summary of the partitioned sections available for the model entity. Figure 3-3 contains simplified summary of the partitioned sections available for the process entity.

PARAMETER	Parameter declarations
VARIABLE	Variable declarations
DISTRIBUTION DOMAIN	Domain declarations
BOUNDARY	Boundary equations
TOPOLOGY	Unit connection equations
EQUATION	Model Equations
INITIAL	Equations

Figure 3-2: Model entity partitioned simplified sections³⁹⁻⁴⁰.

UNIT	Process equipment declarations
SET	Parameter value setting
INITIAL	Initial condition specifications
SOLUTION PARAMETERS	Model based activities specifications
SCHEDULE	Operating policy specifications

Figure 3-3: Process entity partitioned simplified sections³⁹⁻⁴⁰.

In order to describe the simulation activities, the process entity is used. This entity is used to specify what is to be done with the model which contains the mathematical equations of the

system. The information provided by the model is used to specify the simulation activities. gPROMS process entity allows for the model to not suffer any alterations. As explained before the same model can be used to perform activities such as dynamic simulations, optimizations parameter estimation etc. Model parameters can be set at the model entity or set at the process entity. Variables can also be assigned at the process section. An initial section is used to set the values of differential variables such as concentration and surface coverage to zero at time equal to zero. The solution parameters section is used to control various aspects of model-based activities. As well as most modeling software's gPROMS checks for the syntax used in the language, as well as local semantic checking.

3.2.1 Algebraic and Ordinary Differential Equations Solvers

In previous work on electrodeposition models, the mathematical equations solution algorithms need to be implemented in which development time is increased. Since most sources of error from modelers and time consumption in development is involved in solution methods, having an intrinsic independence between mathematical models and solution methods is a great advantage in equation oriented modeling language such as gPROMS.

The system of algebraic and ordinary differential equations is solved using gPROMS proprietary solvers which range from the model based activities of simulation parameter estimation and optimization. Open software architecture is supported in gPROMS; it allows the gPROMS engine gSERVER to be embedded within an external code. Although an open architecture is supported for the mathematical solvers, it was not needed for our approach. The quality of the result and computational effort of solvers can be adjusted by changing error tolerances, default values are chosen which usually lead to good performance for a wide range of problems. Differential equations will use sub solvers for nonlinear and linear equations, this will also need to be specified.

The diffusion flux partial differential equations are solved using IPDAEs (Integral-Partial Differential Algebraic Equation) which is defined within gPROMS environment. Method of lines (MOL) is used to solve the system of IPDAEs numerically. MOL involves the discretization of the distributed equation with respect to all spatial domains. The DASOLV (Differential algebraic equation solver) used as a solver for the solution of mixed sets of differential equations in gPROMS is based on variable time step/variable order Backward Differentiation Formulae (BDF). A second order backward finite difference method is used as the numerical method for the distributed system with a number of finite elements of at least three hundred. The variables of the solvers are restricted to lie within specified lower and upper bounds. In the electrochemical system small variables such as rate constants and concentrations, have an important effect on the system. It is important to distinguish between a concentration of $2.5E-5$ and $1E-4$, and rate constants range from $1E-6$ to $1E-30$. Absolute tolerance for our system was specified to $1E-9$ which handled the simulation and other entities well.

No automatic scaling is handled from the solvers, although scaling of the parameters can affect the solution obtained in either parameter estimation problems or optimization. So scaling of the parameters must be considered. The Linear algebraic equation solver (LASOLVER) used is the MA48 typically used for direct solution of sparse asymmetric linear systems; the algorithmic default parameters are used. In the case of nonlinear algebraic equations they are solved using BDNLSOL which stands for block decomposition nonlinear solver. All variables are restricted to lie within a lower and upper bound.

From the mathematical model equations, the results that best represent the behavior of the system consist of partial current densities of the metals, composition of the metals, efficiencies and surface coverage's all with respect to potential or current. In the case of multilayer deposition, scheduling for different composition of the alloy with different thickness can be

introduced, by varying potential or total current density at scheduled times. Since the process entity uses one model, then various combination of simulation results are available, with changing operating conditions.

3.3 Non General Model Kinetic Parameters

One of the goals of the thesis consists of optimizing kinetic parameters using maximum likelihood estimators instead of trial and error formulation which is time consuming, and not as efficient. Zhuang's model presented a set of parameters for each different concentrations of the alloy as shown in Table 3-3. For cobalt and iron different kinetic parameters need to be used when concentration is changed for the simulation. Trial and error is not efficient in for the estimation for the whole range of concentrations which is a limitation to previous models. In our approach it is intended to use parameter estimation techniques to find a single set of kinetic parameters for all the range of concentrations, so the model can be used as a more general model for electrodeposition studies. For reactions 3,4,5,6 as shown in Zhuang's² model 10 kinetic constants and 10 Inverse Tafel slopes exists since some kinetic parameters need to be replaced for changes in concentrations, where in our approach, only 4 kinetic constants and 4 Tafel slopes will be estimated and used for concentration specified. By developing a more general model, other concentrations, inside the range of concentrations used for estimation can be simulated to find interesting deposition schemes. The trial and error strategy used by Zhuang² and Huang¹⁸ ternary and quaternary model, although gave good results to explain anomalous codeposition behaviors is not practical for studying and using the simulation to explore other behaviors and key variables for different specified concentrations, for fabricating interesting deposition schemes.

Table 3-3: Zhuang's kinetic estimated parameters²

Reactions	Rate constants	Inverse Tafel slopes (V-1)
3	$k_{Co,1} = 2.05 \cdot 10^{-9} \text{ cm} \cdot \text{s}^{-1} \#$	$b_{Co,1} = 13 \#$
	$k_{Co,1} = 1.8 \cdot 10^{-12} \text{ cm} \cdot \text{s}^{-1} \##$	$b_{Co,1} = 20 \##$
4	$k_{Co,2} = 2 \cdot 10^{-9} \text{ mol} \cdot \text{cm}^{-2} \cdot \text{s}^{-1} \#$	$b_{Co,2} = 13 \#$
	$k_{Co,2} = 2 \cdot 10^{-12} \text{ mol} \cdot \text{cm}^{-2} \cdot \text{s}^{-1} \##$	$b_{Co,2} = 20 \##$
5	$k_{Fe,1} = 1.55 \cdot 10^{-25} \text{ cm} \cdot \text{s}^{-1} *$	$b_{Fe,1} = 45 *$
	$k_{Fe,1} = 5.2 \cdot 10^{-32} \text{ cm} \cdot \text{s}^{-1} **$	$b_{Fe,1} = 65 **$
	$k_{Fe,1} = 3.1 \cdot 10^{-27} \text{ cm} \cdot \text{s}^{-1} ***$	$b_{Fe,1} = 55 ***$
6	$k_{Fe,2} = 1 \cdot 10^{-20} \text{ mol} \cdot \text{cm}^{-2} \cdot \text{s}^{-1} *$	$b_{Fe,2} = 45 *$
	$k_{Fe,2} = 5 \cdot 10^{-27} \text{ mol} \cdot \text{cm}^{-2} \cdot \text{s}^{-1} **$	$b_{Fe,2} = 65 **$
	$k_{Fe,2} = 1 \cdot 10^{-22} \text{ mol} \cdot \text{cm}^{-2} \cdot \text{s}^{-1} ***$	$b_{Fe,2} = 55 ***$
<p># Electrolytes in which the Co²⁺ bulk concentration is 0.025 M</p> <p>## Electrolytes in which the Co²⁺ bulk concentration is 0.05 M or 0.1M</p> <p>* Electrolytes in which the Fe²⁺ bulk concentration is 0.025 M</p> <p>** Electrolytes in which the Fe²⁺ bulk concentration is 0.05 M</p> <p>*** Electrolytes in which the Fe²⁺ bulk concentration is 0.1 M</p>		

3.4 Interface Implementation

The Implementation of a front end application for electrodeposition systems is an important adjunct to model based programming. MS Excel and visual basic programming are used to communicate with gPROMS Modelbuilder, thru a gO:Run license. In order to communicate gPROMS with software components which not only provide a graphical interface but also certain computational services at run time, Foreign process interface (FPI) protocol is used. Foreign process and foreign object interfaces are used to exchange data with external software. MS Excel software protocol is available for gPROMS where the supported device such as foreign objects and foreign processes is used. Not only are the parameters used in the model accessed thru MS Excel, but the output results are stored and accessed by MS Excel.

3.4.2 Implementation of Front End Application

In order to communicate gPROMS modelbuilder with the excel front end application a gPROMS runtime object license (gO:Run) is needed. It is an execution only engine needed to run simulation and parameter estimation model. For the case of our electrodeposition system foreign object is used to input values for the parameters directly from MS Excel. Parameters will not have to be modified inside gPROMS which facilitates the study of the system directly from the front end application.

Foreign process interface is used with gPROMS “GET” task where simulation results are stored in Excel worksheets where the cells are used to automatically graph all the results as defined by the user. Excel spreadsheet contains all current density calculations with respect to potential, as well as composition and current efficiency. Subjacent worksheets contain experimental data comparisons as well as surface coverage results. Visual Basic is used to execute the simulation as well as to stop it. A macro containing programming code has been

implemented in order to show experimental data available depending on concentrations specified. This is used to compare the results from simulation to the experimental data results.

3.4.3 Application and Functionality

The features of the graphical user interface are there to interact with key variables to execute the simulations. The buttons used to execute while using the front end application are the following

- START used to execute the simulation after concentrations of interest and other key variables have been modified.
- STOP used to stop the simulation at any time.
- CLEAR results from previous simulation runs, or experimental data comparisons can be cleared although it is not necessary to clear the data since a new simulation replaces the previous results
- EXP DATA as an additional feature of the interface when concentrations are specified, the buttons allows users to compare experimental data to simulation results in order to study if simulation mimics experimental findings.

The following figure 3-4 contains a template of the front end application interface. Results such as surface coverage, side reaction and other simulation results of interest are found by scrolling down through the interface. Figure 3-5 contains a simulation study for an alloy consisting of nickel 0.2M, cobalt 0.025M and iron 0.05M, where results for surface coverage are seen.

3.4.4 Goals and Importance

As mentioned before the implementation of a front end application of electrodeposition systems is an important adjunct to model based programming. It provides non-modeling users the advantage to study the results and knowledge of the model without worrying about model

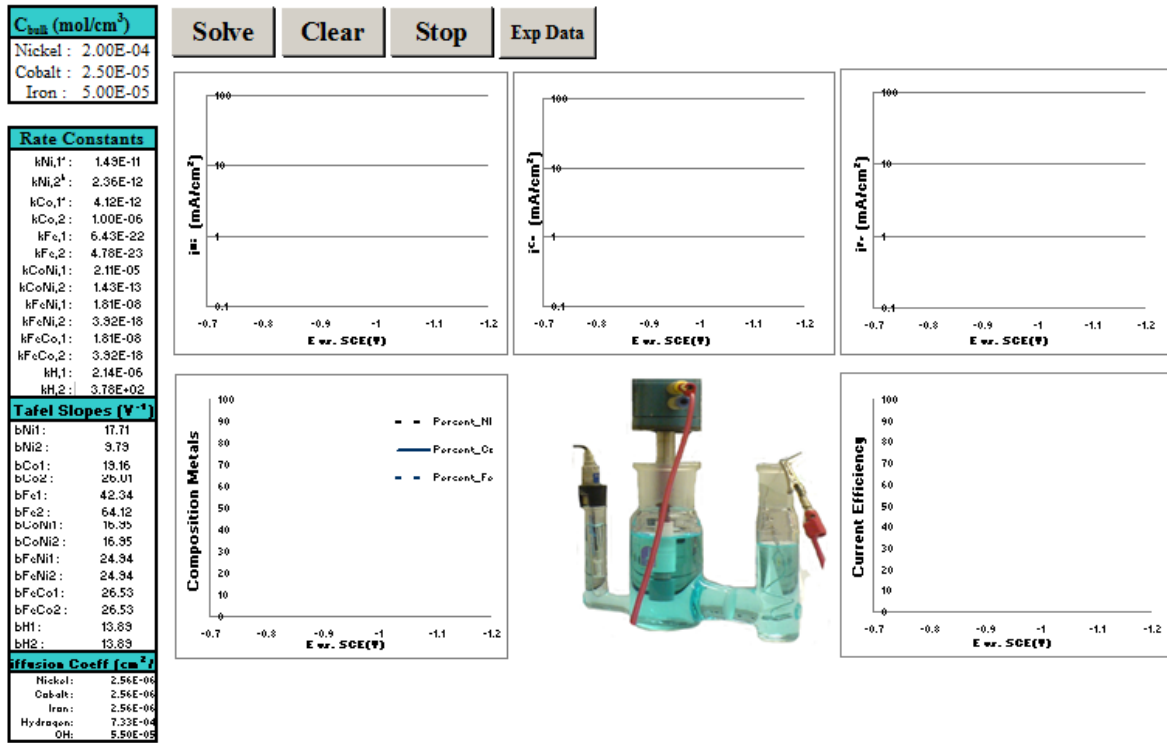


Figure 3-4: Front end interface implementation.

equation solvers or programming language. It also provides protection to the model from unauthorized change since it can be encrypted to protect confidential information. Most importantly it increases the reusability of the model since knowledge can be transferred easily between different researchers. The interface can be expanded for different systems containing more reactions, where non programming users, can study effects of key variables such as concentrations, and study the importance of kinetic parameters.

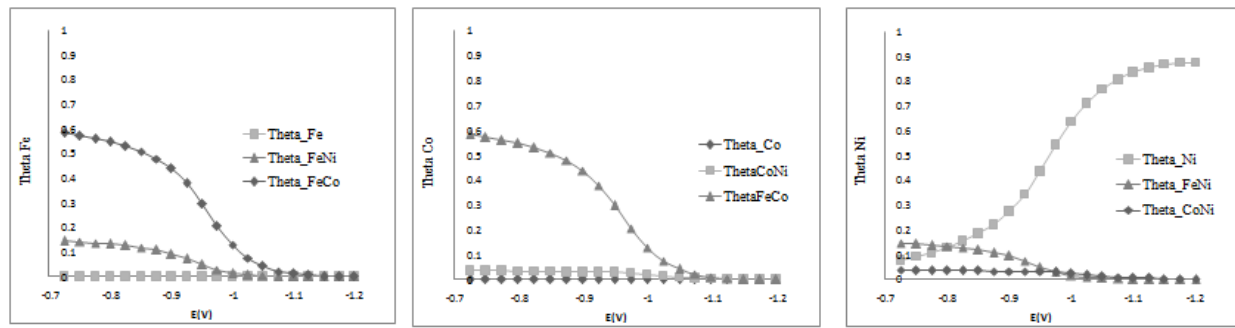
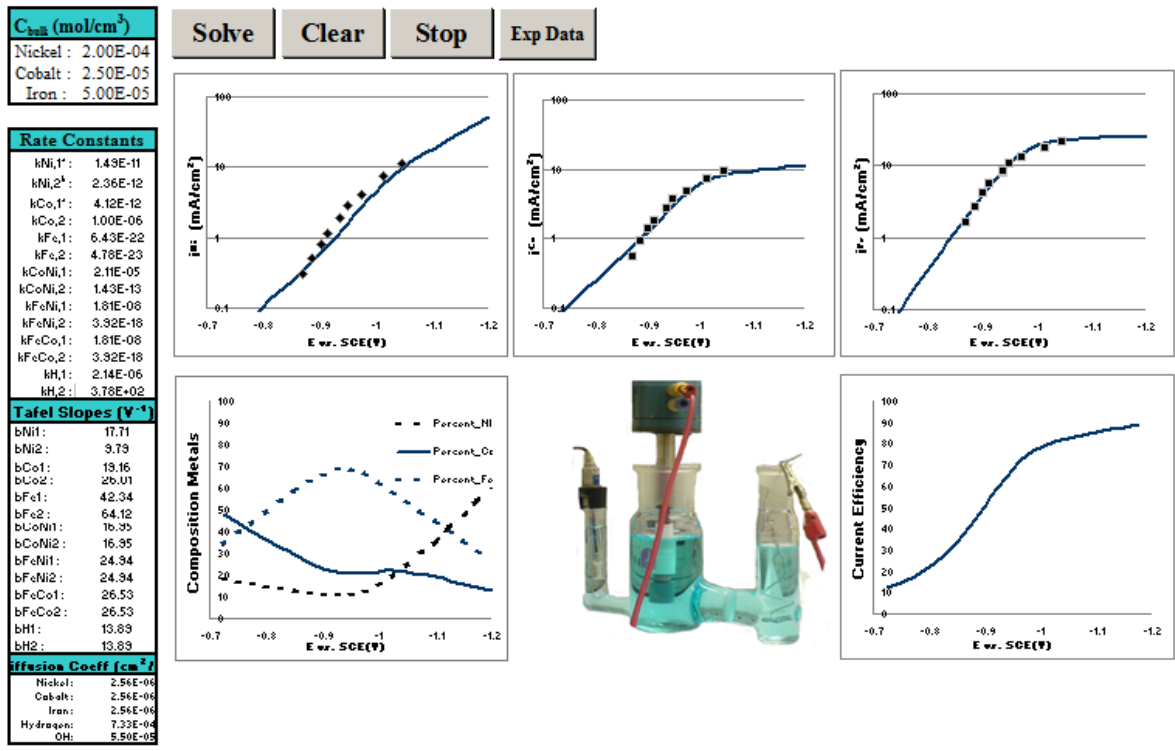


Figure 3-5: Executed front end interface implementation

Simulations can be performed for a number of interesting studies where anomalous codeposition behavior has been found to be simulated using the mixed metal intermediate reactions to account for catalytic effects on the less noble metal deposition by the more noble metal. Both Zhuang and Huang dissertations, contain simulation results for enhancements and inhibition effects. The experimental and simulation results studied the effect of rotation rates,

electrolyte concentration, bulk pH on the metal partial current densities, compositions, and current efficiencies. More experimental results to show the capabilities of the model are explained in Chapter 4 after one single set of parameters for all concentrations of the alloy is estimated using parameter estimation techniques.

CHAPTER 4. PARAMETERS ESTIMATION

In the previous chapter the mathematical model is implemented for simulations at different operating conditions where the developed mechanism is intended to mimic the experimental behavior. This chapter will focus on testing the maximum likelihood estimator, to attempt to find the best fit for our experimental data consisting of partial current densities of the metals versus potential at different concentrations of the alloy. The parameters which will be estimated will consist of the kinetic parameters used in Tafel approximations of the current densities. Both models will be used for parameter estimation.

4.1. Introduction

Parameter estimation, also called data regression is an important step involved in the formulation and validation of mathematical models. Given the governing equations of the model and a set of experimental data, the problem is to find and estimate the unknown model parameters so that the model results mimic the data in some optimal matter. This determination of values for the adjustable parameters is the objective of parameter estimation studies. Parameter estimation is essentially an optimization problem, where suitable objective functions are used. Efficient and robust methods have been developed over time from the structure of objective functions. Specific issues relate to parameter estimation problems such as:

- The structure of the model: defined for algebraic and differential equation models as well as for linear or nonlinear models.
- Objective function selection: refers to a scalar function with dependence to the chosen parameters. The choice of the objective function dictates the value of the estimates as well as the statistical properties.
- Solution techniques: developed for specific algorithms and methods to minimize or maximize the objective function.

- Statistical properties: uncertainty in model parameters as well as in calculated values.
- Model adequacy: validations to how good the model responds to the system.

The mentioned issues are addressed in estimation formulations for determination of the adjustable models in steady state and dynamic systems represented by algebraic and differential equation models.

A popular statistical method used in many applications is the maximum likelihood estimation (MLE). The maximum likelihood estimators have been shown under normal conditions, to be consistent and asymptotically efficient⁴¹, which justify its use in a large variety of applications. It has been found useful in aiding in mathematically modeling of phenomena and the estimation of constants in models.

4.2 Parameter Estimation Mathematical Formulation

Various elements of the parameter estimation problem are introduced considering the mathematical model implementation of the electrochemical system. In terms of our specific application, a considerable number of parameters, such as kinetic parameters are involved in the model of this complex system under study. We will rely on the maximum likelihood theory and will require a specifically generated set of experimental data. Consequently, in our approach, a validation step will be undertaken in conjunction with the execution of parameter estimation studies. In our formulation we propose the following general mathematical definition for the estimation problem:

$$\min_{\theta, \beta, \omega, \gamma} \varphi(\tilde{z}(t), z(t), \sigma(t)) \quad [4.1]$$

$$F(\dot{x}(t), x(t), y(t), u(t), p, \theta, \beta) = 0, t \in [0, t_f] \quad [4.2]$$

$$I(\dot{x}(0), x(0), y(0), u(0), p, \theta, \beta) = 0 \quad [4.3]$$

$$\sigma(t) = \sigma(\tilde{z}(t), z(t), \omega, \gamma), t \in [0, t_f] \quad [4.4]$$

With

$$\theta^{min} \leq \theta \leq \theta^{max} \quad [4.5]$$

$$\beta^{min} \leq \beta \leq \beta^{max} \quad [4.6]$$

$$\omega^{min} \leq \omega \leq \omega^{max} \quad [4.7]$$

$$\gamma^{min} \leq \gamma \leq \gamma^{max} \quad [4.8]$$

where $\varphi(t)$ is a generic objective function. The symbol Z designates our experimental observations and will be considered explicitly in the objective function. The decision variables of the estimation problem are the vectors θ , ω , β and γ ; note that these parametric variables correspond to different features of the overall mathematical model, for example θ , are our kinetic parameters which need to be estimated using the experimental data, ω and γ are associated with the statistical information about the experimental observations. $F(\cdot)$ and $I(\cdot)$ denote, in general, the set of partial differential algebraic equations encompassing the fundamental process model and the set of initial conditions respectively. In these equations x and y denote the differential and algebraic variables respectively, in addition $u(t)$ are the set of input variables. Additionally, the variable $\sigma(t)$, which is *intrinsic* to the objective function, will be an explicit function of the model predictions $z(t)$, the experimental observations $\tilde{z}(t)$, and the parametric variables ω and γ . Depending on the nature of $\varphi(t)$, $\sigma(t)$ can either be the variance of the measurement errors or, simply, the weight of individual variables within this multivariable objective function.

4.3 Objective Function Maximum Likelihood Estimator

The maximum likelihood objective function attempts to determine the optimal values for the kinetic unknown parameters θ , as mentioned before, in order to maximize the probability that the results obtained from experiments fit the mathematical model output. The form of the objective function is determined by a series of implicit and explicit assumptions made while defining a given parameter estimation problem. For instance, maximum likelihood (ML)

estimation makes use of the information on the statistical distribution of the observations to derive an expression of the objective function. Assuming, that the random measurement errors are additive, independent and normally distributed, with zero mean and constant standard deviation, and the independent variables and unknown parameters are non-random, then the following objective function gives a *maximum likelihood estimator*⁴⁰:

$$\begin{aligned} \varphi_{ML}(\tilde{z}, z(t), \sigma(t)) &= \frac{1}{2} \cdot \varphi_{ML} \\ &= \frac{N}{2} \ln(2\pi) + \frac{1}{2} \min_{\Theta} \left(\sum_{i=1}^{NE} \sum_{j=1}^{NV_i} \sum_{k=1}^{NM_{ij}} \left[\ln(\sigma_{ijk}^2) + \frac{(\tilde{z}_{ijk} - z_{ijk})^2}{\sigma_{ijk}^2} \right] \right) \end{aligned} \quad [4.9]$$

Where N equals the total number of measurements during all experiments, NE equals the number of experiments performed NV_i the number of variables measured in the *i*th experiment and NM_{ij} the number of measurements of the *j*th variable in the *i*th experiment.

The general form of the variance model is

$$\sigma^2 = \sigma^2(\beta, z, \tilde{z}) \quad [4.10]$$

For this study a constant variance is used for experimental data measurements where: $\sigma^2 = \omega^2$. Experimental measurement variances are found for current densities and used for the estimation.

4.4 Parameter Estimation Execution Solver

The gEST Parameter estimation tool of gPROMS package is used to solve the maximum likelihood optimization problem. MXLKHD solver is used, where the global optimum is found by applying sequential quadratic programming (SQP) method. It calculates the objective function gradient with respect to the parameters to be estimated, and follows by using this first derivative information to determine the search direction. Therefore it is considered an indirect solver. The algorithm takes advantage of the DASOLV solver for solution of the underlying differential

algebraic equation problem as well as the sensitivities computation. Optimization tolerance is important to specify where a criterion needs to be satisfied to reach convergence.

Because kinetic parameters rate constants and Tafel slopes vary significantly in magnitude which can affect the performance of the optimization algorithms an appropriate scaling of the equations is implemented. A general mathematical form shown in equation 4.11 to 4.13 is used for scaling. According to the ranges of the parameters the scaled parameters vary between -1 and 1. It is known that for default non-scaling to take place d_j and c_j have to equal 1 and 0 respectively⁴⁰.

$$\tilde{\theta}_j = \frac{\theta_j - c_j}{d_j} \quad [4.11]$$

$$d_j = \frac{1}{2}(\theta_j^{max} - \theta_j^{min}) \quad [4.12]$$

$$c_j = \frac{1}{2}(\theta_j^{max} + \theta_j^{min}) \quad [4.13]$$

4.5 Estimation of Optimal Kinetic Parameter Strategy

To increase the efficiency of the maximum likelihood execution a specifically generated set of experimental data is required. For estimation purposes of this thesis, the experimental work from Zhuang² on ternary alloy system and Huang¹⁸ quaternary system will be used. Experimental data contains several electrolyte compositions, where deposition current densities of the metals are found for changes in potential or current. Table 4-1 contains the experimental data concentrations that will be used and the parameters which will be estimated with this data. To be able to reduce computational effort, and be able to fine tune the parameters precisely using the right set of data and variances, a strategy is imposed. First single metal deposition kinetic parameters will be estimated using the single metal deposition experimental data. Once the single deposition kinetic data is known it will be imputed into the model. Then the alloy mixed metal

kinetic parameters will be estimated using alloy experimental data which contain five different electrolyte compositions of the alloy available for the estimation. The number of kinetic parameters will depend on the mechanism chosen for the reactions. Side reaction kinetic parameters will be estimated using the data from single metal and alloy depositions.

Table 4-1: Kinetic parameters estimated using various electrolyte compositions for single and alloy depositions

Deposition	NiSO ₄	CoSO ₄	FeSO ₄	H ₃ BO ₃	Na ₂ SO ₄	Estimated Parameters
Ni	0.2M			0.4 M	0.55 M	$k_{Ni,1}, k_{Ni,2}, b_{Ni,1}, b_{Ni,2}$
Co		0.025 M		0.4 M	0.725 M	$k_{Co,1}, k_{Co,2}, b_{Co,1}, b_{Co,2}$
Co		0.05 M		0.4 M	0.7 M	
Co		0.1 M		0.4 M	0.65 M	
Fe			0.025 M	0.4 M	0.725 M	$k_{Fe,1}, k_{Fe,2}, b_{Fe,1}, b_{Fe,2}$
Fe			0.05 M	0.4 M	0.7 M	
Fe			0.1 M	0.4 M	0.65 M	
NiCoFe	0.2 M	0.025 M	0.025 M	0.4 M	0.5 M	$k_{CoNi,1}, k_{CoNi,2}, b_{CoNi,1}, b_{CoNi,2}$
NiCoFe	0.2 M	0.05 M	0.025 M	0.4 M	0.475 M	
NiCoFe	0.2 M	0.1 M	0.025 M	0.4 M	0.425 M	
NiCoFe	0.2 M	0.025 M	0.025 M	0.4 M	0.5 M	$k_{FeNi,1}, k_{FeNi,2}, b_{FeNi,1}, b_{FeNi,2}$
NiCoFe	0.2 M	0.025 M	0.05 M	0.4 M	0.475 M	$k_{FeCo,1}, k_{FeCo,2}, b_{FeCo,1}, b_{FeCo,2}$
NiCoFe	0.2 M	0.025 M	0.1 M	0.4 M	0.425 M	

4.6 Parameter Estimation Study for Single Metal and Alloy Deposition

Single metal depositions estimations are performed in order to estimate kinetic parameters involved in two step manner reactions. The mathematical definition considers a process described by algebraic and mixed differential equations. Process entity which is used for simulation contains model information which is taken from the parameter estimation entity. The following variables are used for the estimation:

- C : differential variables

- θ, δ, W, i : algebraic variables
- C_{bulk}, P : time invariant control variables
- b, k : unknown variables to be estimated

The experimental entity needs to be specified. Statistical constant variance is specified for current density values. Results will depend strongly on the standard deviation of the measurement errors. The parameter estimation entity is then specified. The following table 4-2 contains the specification for all single metal estimations needed in the parameter estimation entity such as lower and upper bounds. Experimental runs are also selected in order to run the estimation specified in Table 4-1 for each kinetic parameter. The estimation of the metals is performed in separate strategic runs as mentioned before. The final optimal value results from the estimation of single metal deposition kinetic parameters are the following from table 4-2.

Table 4-2: Parameter estimation specifications and results for single metal deposition

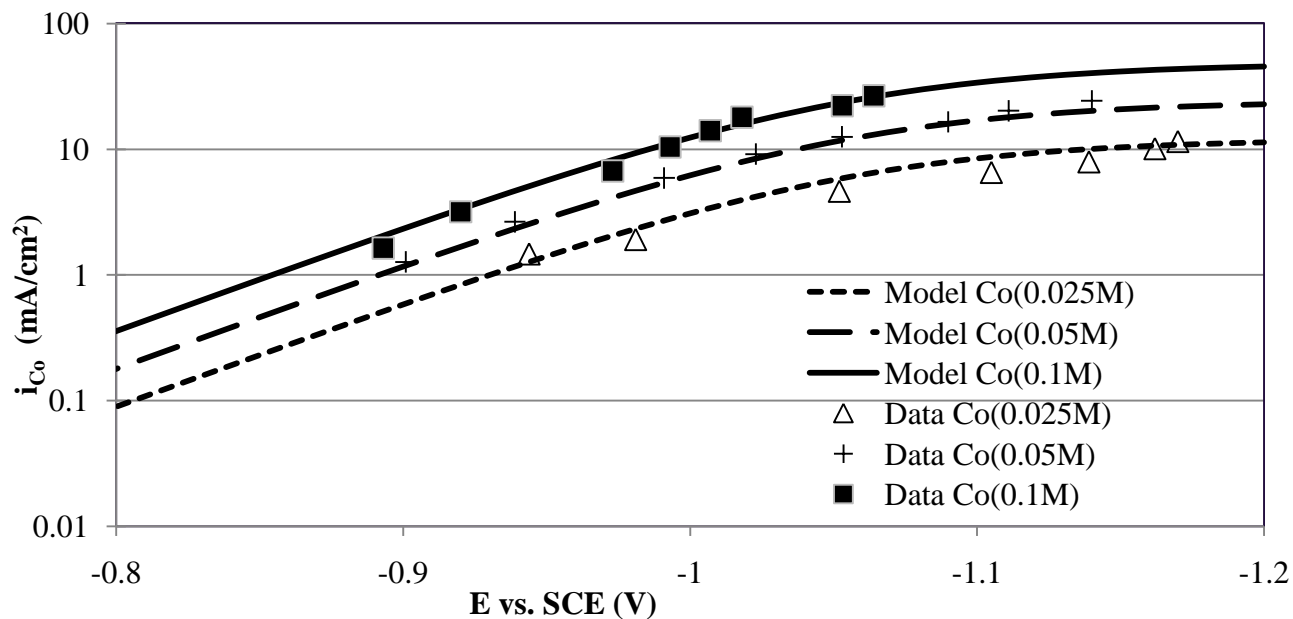
Parameter Estimates	Final Optimal Value	Lower Bound	Upper Bound
$k_{\text{Ni},1} (\text{cm}\cdot\text{s}^{-1})$	1.49E-11	1.00E-15	1.00E-05
$k_{\text{Ni},2} (\text{mol}\cdot\text{cm}^{-2}\cdot\text{s}^{-1})$	2.36E-12	1.00E-15	1.00E-05
$b_{\text{Ni},1} (\text{V}^{-1})$	17.71	5	25
$b_{\text{Ni},2} (\text{V}^{-1})$	9.79	5	25
$k_{\text{Co},1} (\text{cm}\cdot\text{s}^{-1})$	4.12E-12	1.00E-30	1.00E-04
$k_{\text{Co},2} (\text{mol}\cdot\text{cm}^{-2}\cdot\text{s}^{-1})$	1.00E-06	1.00E-30	1.00E-04
$b_{\text{Co},1} (\text{V}^{-1})$	19.16	1	60
$b_{\text{Co},2} (\text{V}^{-1})$	26.01	1	60
$k_{\text{Fe},1} (\text{cm}\cdot\text{s}^{-1})$	6.43E-22	1.00E-32	1.00E-16
$k_{\text{Fe},2} (\text{mol}\cdot\text{cm}^{-2}\cdot\text{s}^{-1})$	4.78E-23	1.00E-32	1.00E-16
$b_{\text{Fe},1} (\text{V}^{-1})$	42.34	40	80
$b_{\text{Fe},2} (\text{V}^{-1})$	64.12	40	80
$k_{\text{Cu},1} (\text{cm}\cdot\text{s}^{-1})$	9.99E-07	1.00E-12	1.00E-04
$b_{\text{Cu},1} (\text{V}^{-1})$	44.05	20	80

An overlay plot using the optimal parameter estimates are shown for cobalt, iron, nickel and copper in figure 4-1. The partial current densities simulation mimics the experimental data successfully, providing a graphical validation of the estimates. The front end electrodeposition application is used to simulate the single metal depositions, while setting the other metals to zero. Figure 4-1 shows the single metal partial current densities at different bulk concentrations of 0.1M, 0.05M and 0.025M for iron and cobalt. For nickel and copper a single bulk concentration of 0.2M and 0.001M are used respectively. With an increase in the bulk concentration of cobalt the partial current density increases, and seems to approach its limiting value at potentials more negative than -1.15 V. With an increase in the bulk concentration iron the partial current density increases, and for concentrations of 0.05M and 0.1M it seems to approach its limiting value at potentials more negative than -1.05 V. For nickel the regions shown from -0.8 to -1.2V are kinetically controlled, the limiting value is reached at values more negative than -1.2V. As for copper the kinetically controlled region is from -0.1 to -0.25 V approximately and then approaches its limiting value at potentials more negative than -0.2 V.

Using the optimum estimated kinetic parameters from table 4.2 the mixed metal alloy deposition kinetic parameters can be estimated. Mixed metal kinetic parameters are estimated in separate runs strategically using experimental data as shown in table 4.1. Lower and upper bound values used for estimations of mixed metal and side reaction kinetic parameters as well as the optimal estimates found from the execution of the entity are shown in table 4.3. Using the estimated parameters for alloy deposition an overlay plot of the partial current densities using the optimal parameter estimates is shown in figure 4-2 compared to the experimental data. The side reaction partial current density is compared to its experimental data in figure 4-3. The plots show an agreement of the experimental data with the simulation results. The alloy simulations are performed using the front end electrodeposition application, having the previous estimated single

metal kinetic parameter estimates, and adding the new optimal mixed metal kinetic parameters needed for alloy deposition.

(a)



(b)

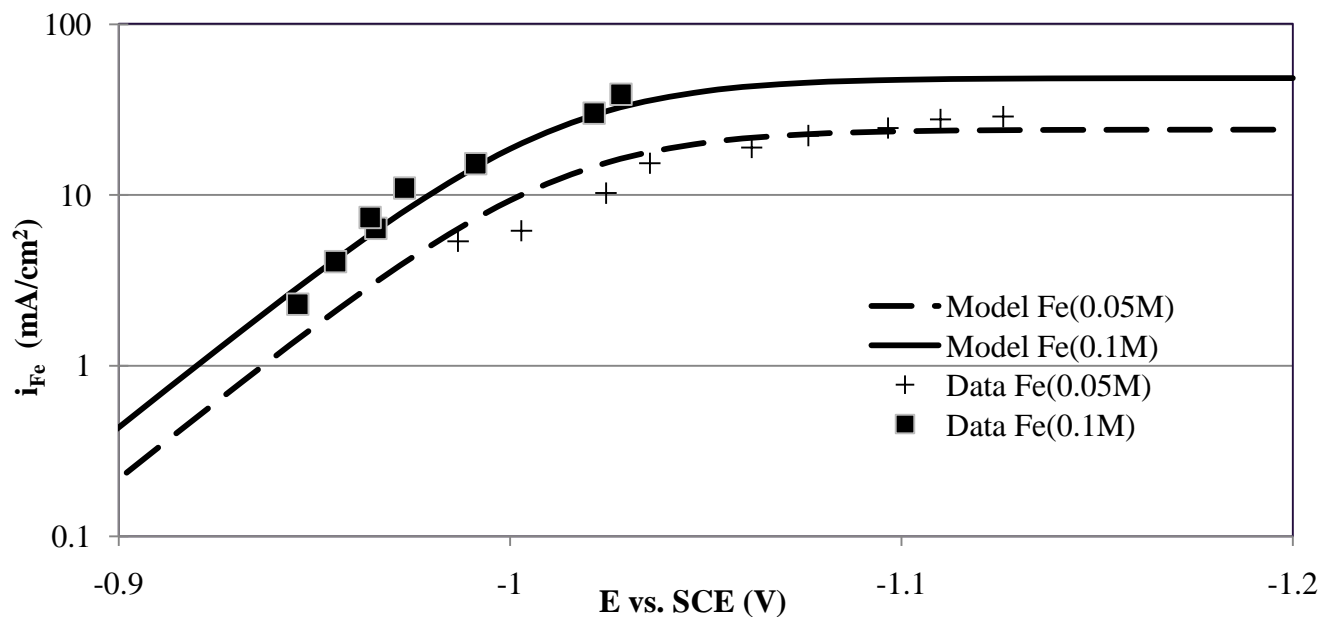
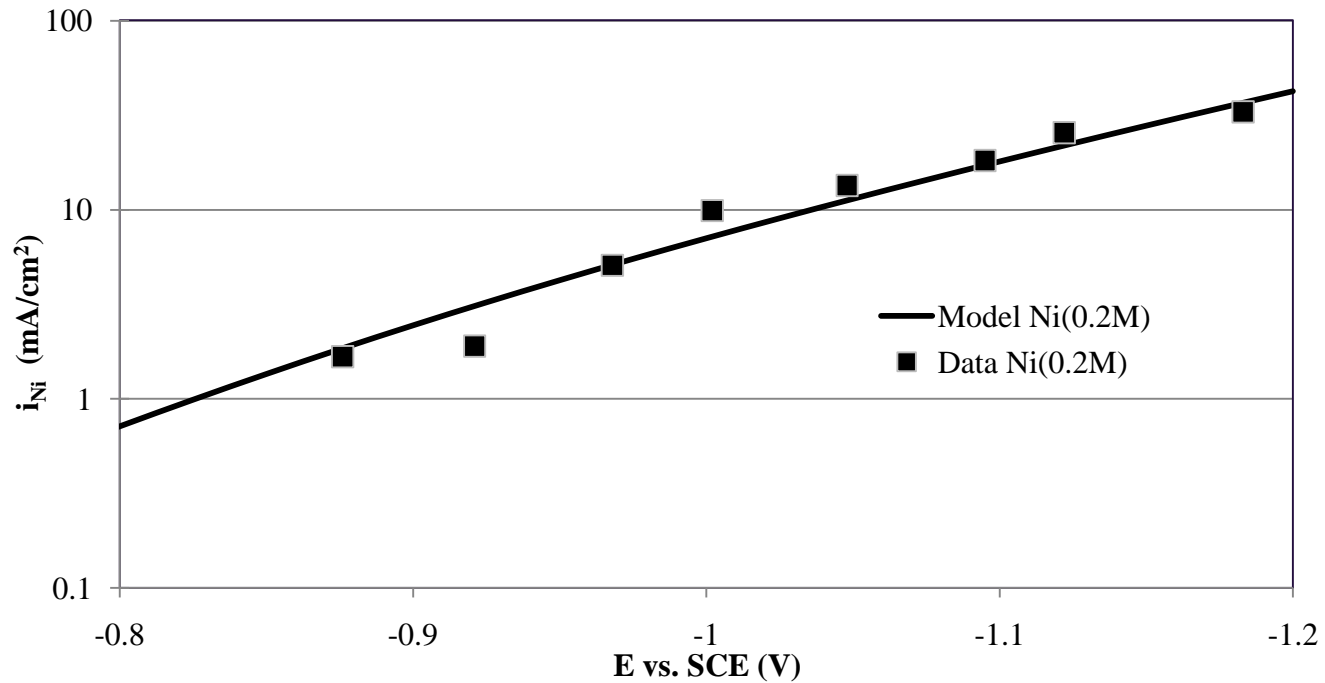
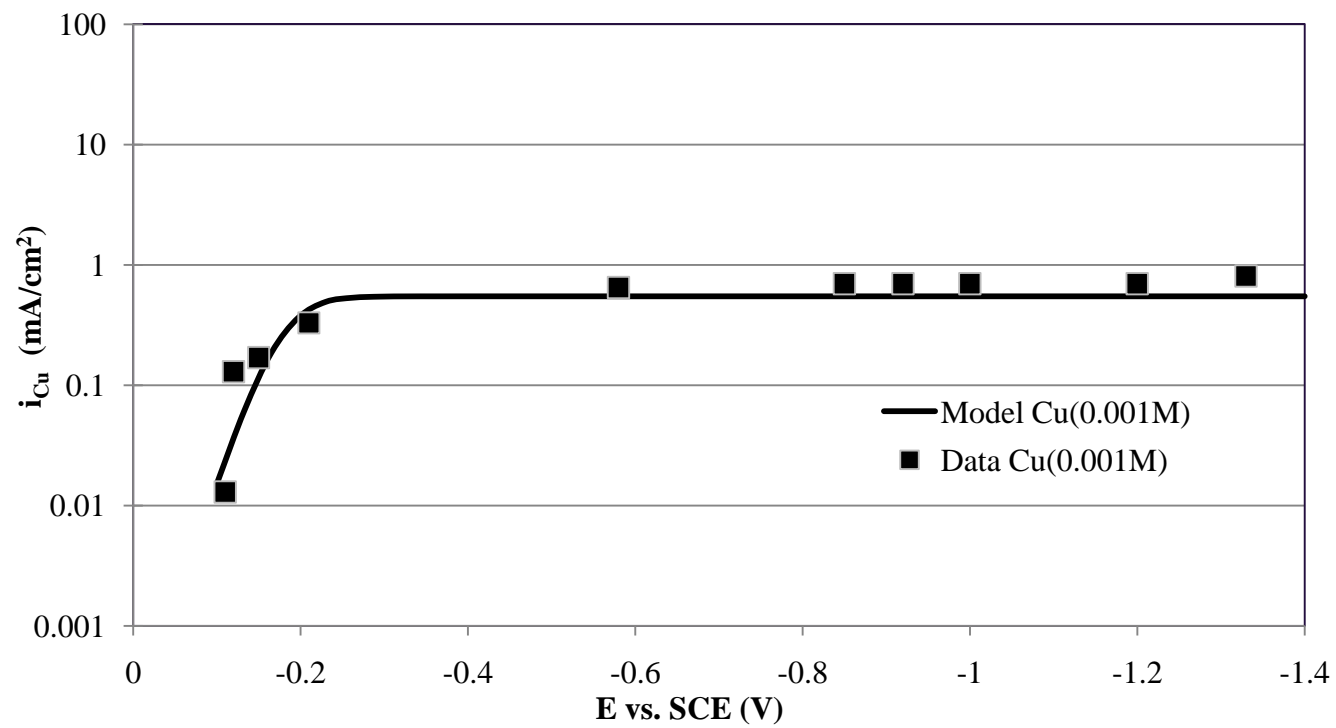


Figure 4-1: Simulated (a) Co (b) Fe (c) Ni (d) Cu single metal deposition partial current density using optimal kinetic parameters. (Fig. 4-1 continued)

(c)



(d)



Using the optimum estimated kinetic parameters from table 4.2 the mixed metal alloy deposition kinetic parameters can be estimated. Mixed metal kinetic parameters are estimated in separate runs strategically using experimental data as shown in table 4.1. Lower and upper bound values used for estimations of mixed metal and side reaction kinetic parameters as well as the optimal estimates found from the execution of the entity are shown in table 4.3. Using the estimated parameters for alloy deposition an overlay plot of the partial current densities using the optimal parameter estimates is shown in figure 4-2 compared to the experimental data. The side reaction partial current density is compared to its experimental data in figure 4-3. The plots show an agreement of the experimental data with the simulation results. The alloy simulations are performed using the front end electrodeposition application, having the previous estimated single metal kinetic parameter estimates, and adding the new optimal mixed metal kinetic parameters needed for alloy deposition.

For the alloy, the partial current density of cobalt increases as its concentration increases from 0.025M to 0.1M. The dominant kinetically controlled region is found for potentials more positive than -1V. At more negative than -1V the rate appears to approach its limiting value. The partial current density of iron appears to not be affected by the change in iron concentration for the kinetically controlled region from potentials more positive than -1V. For potentials more negative than -1.1V the rate approaches its limiting value, where there is an increase in the rate for an increase in the concentration from 0.025M to 0.1M. Figure 4-3 shows the simulated partial current density for the side reaction, for various concentrations of the alloy. The rate increases with an increase in the concentrations of cobalt and iron until it reaches its limiting value where it is not affected by the change in concentrations. Hydrogen absorption is very low, on the order of 10^{-9} .

Table 4-3: Parameter estimation specifications and results for alloy deposition

Parameter Estimates	Final Optimal Value	Lower Bound	Upper Bound
$k_{\text{CoNi},1}$ ($\text{cm}^4\text{mol}^{-1}\text{s}^{-1}$)	2.11E-05	1.00E-09	1.00E-04
$k_{\text{CoNi},2}$ ($\text{mol cm}^{-1}\text{s}^{-1}$)	1.43E-13	1.00E-17	1.00E-12
$b_{\text{CoNi},1}$ (V^{-1})	16.95	16	24
$b_{\text{CoNi},2}$ (V^{-1})	16.95	16	24
$k_{\text{FeNi},1}$ ($\text{cm}^4\text{mol}^{-1}\text{s}^{-1}$)	1.81E-08	1.00E-11	1.00E-07
$k_{\text{FeNi},2}$ ($\text{mol cm}^{-1}\text{s}^{-1}$)	3.92E-18	1.00E-22	1.00E-17
$b_{\text{FeNi},1}$ (V^{-1})	24.94	22	32
$b_{\text{FeNi},2}$ (V^{-1})	24.94	22	32
$k_{\text{FeCo},1}$ ($\text{cm}^4\text{mol}^{-1}\text{s}^{-1}$)	1.81E-08	1.00E-11	1.00E-07
$k_{\text{FeCo},2}$ ($\text{mol cm}^{-1}\text{s}^{-1}$)	3.92E-18	1.00E-22	1.00E-17
$b_{\text{FeCo},1}$ (V^{-1})	26.53	22	32
$b_{\text{FeCo},2}$ (V^{-1})	26.53	22	32
$k_{\text{H},1}$ ($\text{cm}\cdot\text{s}^{-1}$)	2.14E-06	1.00E-10	1.00E-04
$k_{\text{H},2}$ ($\text{cm}\cdot\text{s}^{-1}$)	3.78E+02	1	6.00E+02
$b_{\text{H},1}$ (V^{-1})	13.89	5	20
$b_{\text{H},2}$ (V^{-1})	13.89	5	20

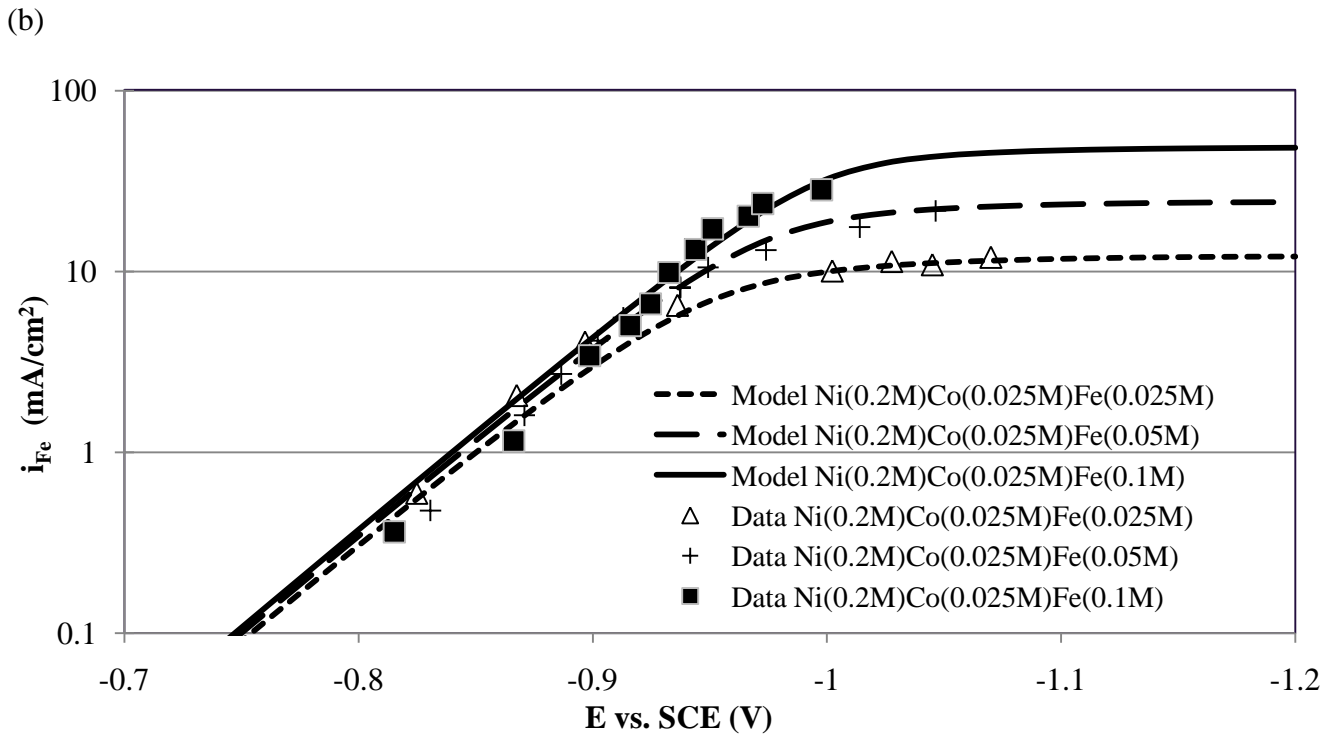
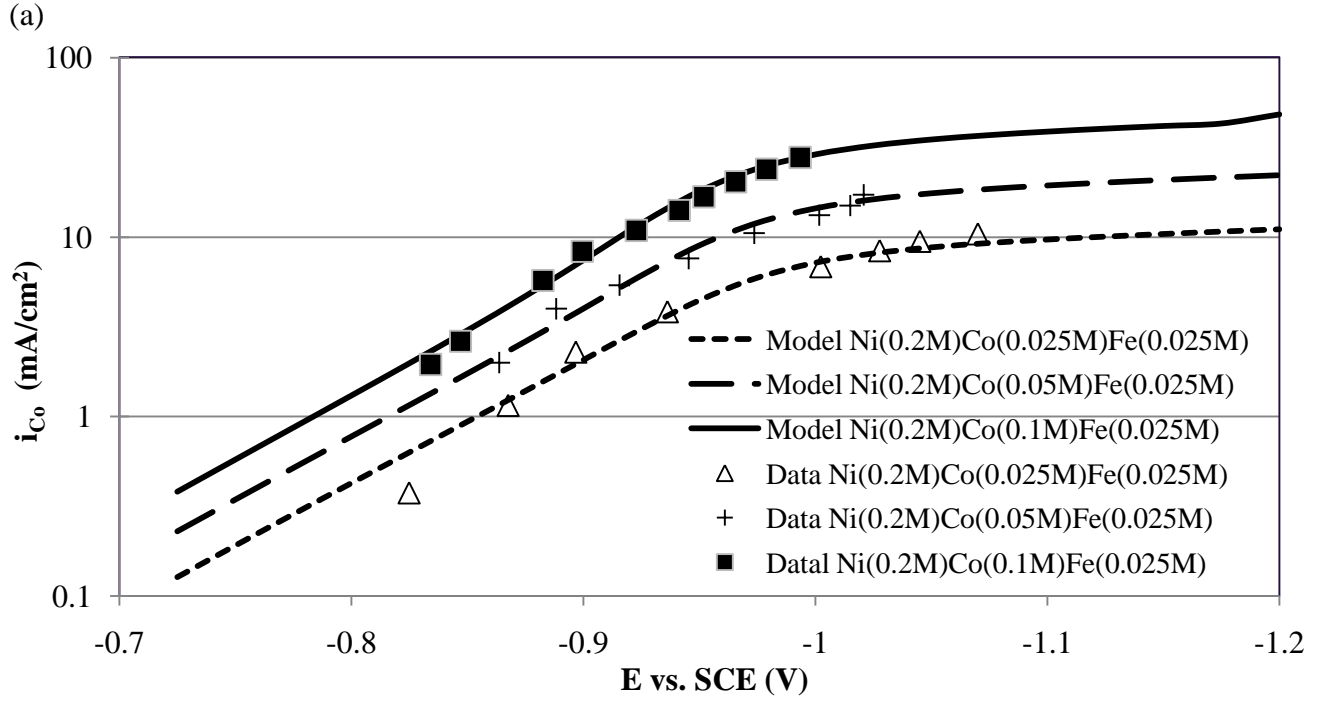


Figure 4-2: Simulated (a) Co and (b) Fe partial current density during alloy metal deposition using optimal kinetic parameter estimates.

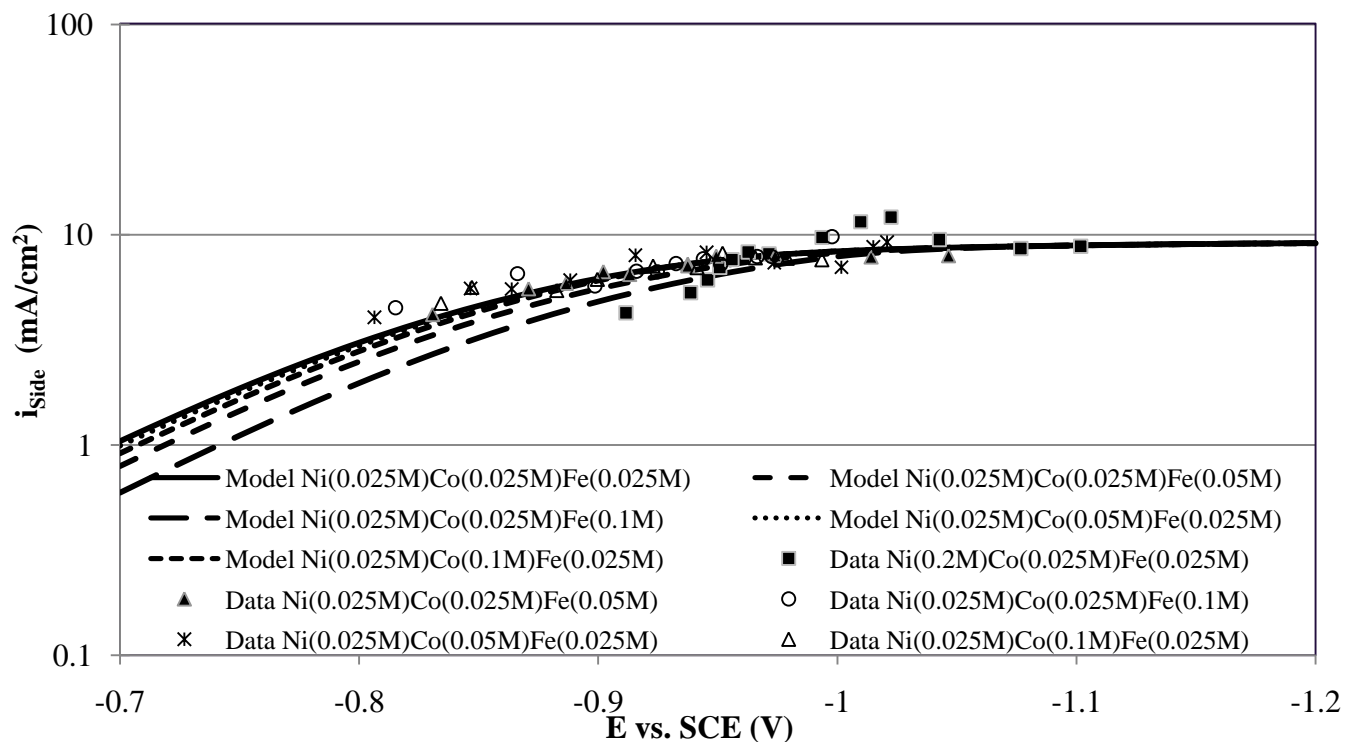


Figure 4-3: Simulated side reaction partial current density during alloy metal deposition using optimal kinetic parameter estimates.

4.7 Capabilities of the Electrodeposition Model

It has been shown that parameter estimation techniques such as the maximum likelihood estimator, works efficiently to estimate kinetic parameters such as rate constants and Tafel slopes for complex reactions involved in electrodeposition systems. Trial and error techniques did not facilitate the opportunity to find a single set of parameters for changes in concentrations. Now that a single set of parameters is available the model can be used for studying the process, as well as fabricating interesting compositions of alloys. Concentration changes can be simulated to show inhibition and enhancement effects from alloy and single metal depositions. pH effects on side reactions can be also simulated as well as results showing deconvolution of the metal partial currents and surface coverage of the metal species.

Figure 4-4 shows enhancement effects, where the iron alloy rate is enhanced compared to its single metal deposition. The enhancement is dependent on the concentration of the metals. With increasing iron bulk concentrations 0.05M to 0.1M the enhancement is reduced where the single iron deposition moves to a more positive potential. The alloy iron rate reaches its limiting value at potentials more negative than -1.05 V. Figure 4-5 shows inhibition effects, where the nickel rate is inhibited compared to its single metal deposition. The inhibition is present when the potential is more positive than -1.1V. For potentials more negative than -1.1 V the nickel rate reaches its limiting value, where the alloy rate is no longer inhibited. The inhibition is also greater for an increase in the iron bulk concentration from 0.025M to 0.08M. The reaction mechanisms are able to simulate inhibition and enhancement effects of anomalous codeposition behavior. By changing the concentration of the electrolyte further studies can be accomplished to study anomalous codeposition behavior as shown in Zhuangs and Huang's dissertations³³⁻³⁴.

(a)

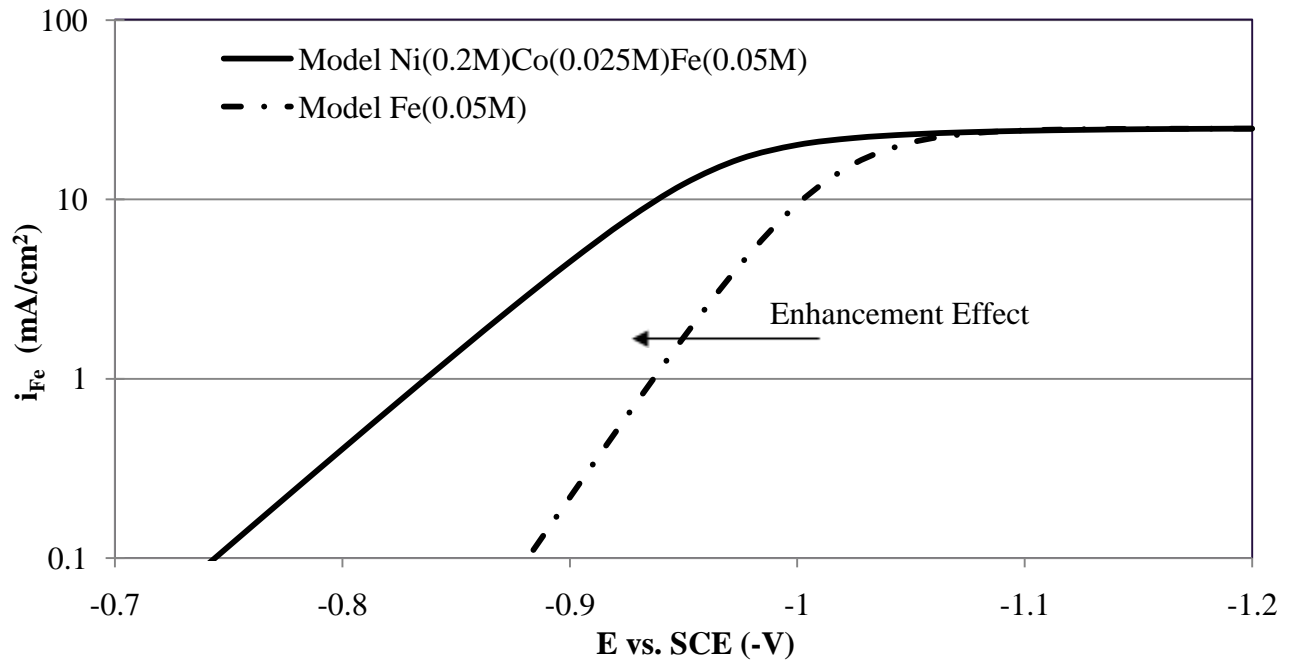


Figure 4-4: Enhancement effect simulation for iron partial current at a concentration of single metal deposition of (a) 0.05M (b) 0.1M and ternary alloy deposition. (Fig. 4-4 continued)

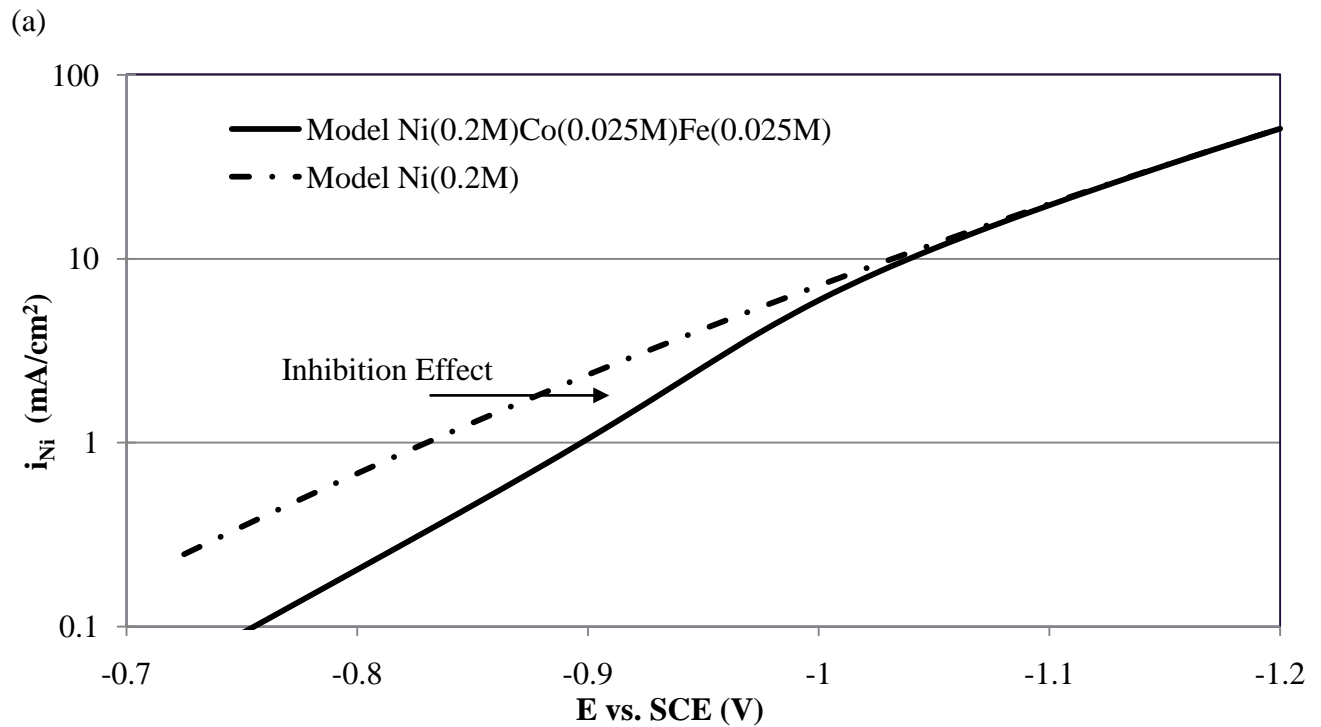
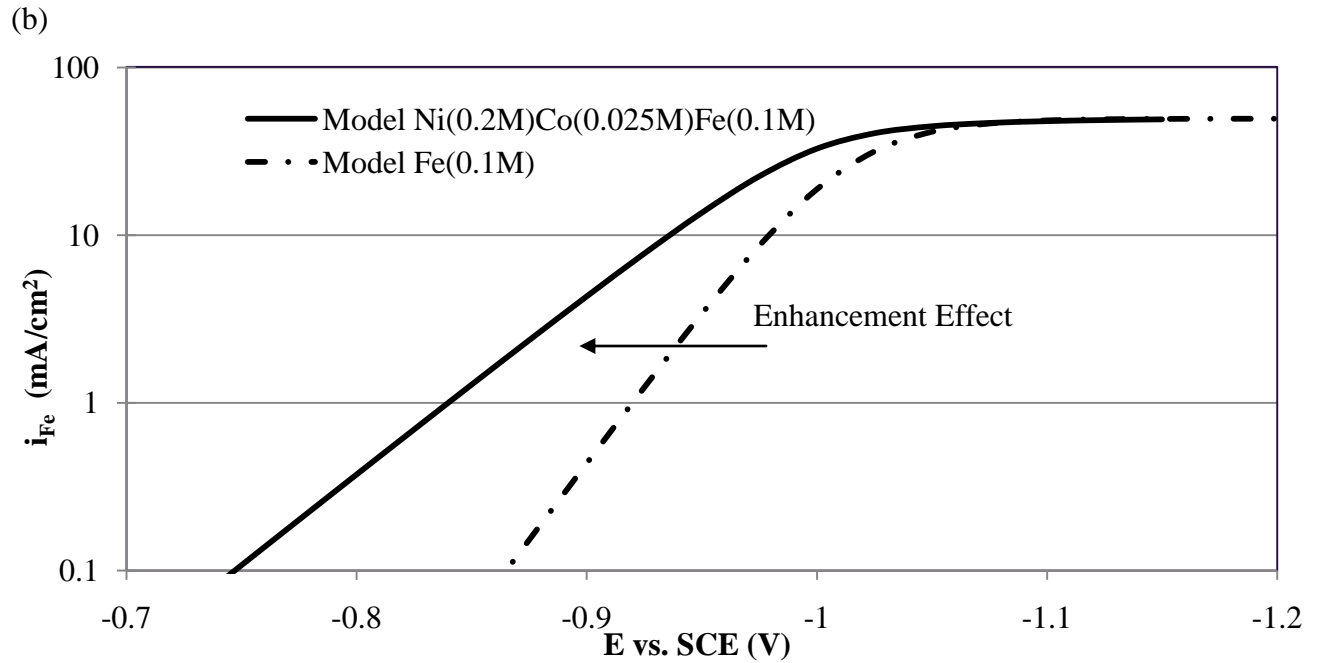
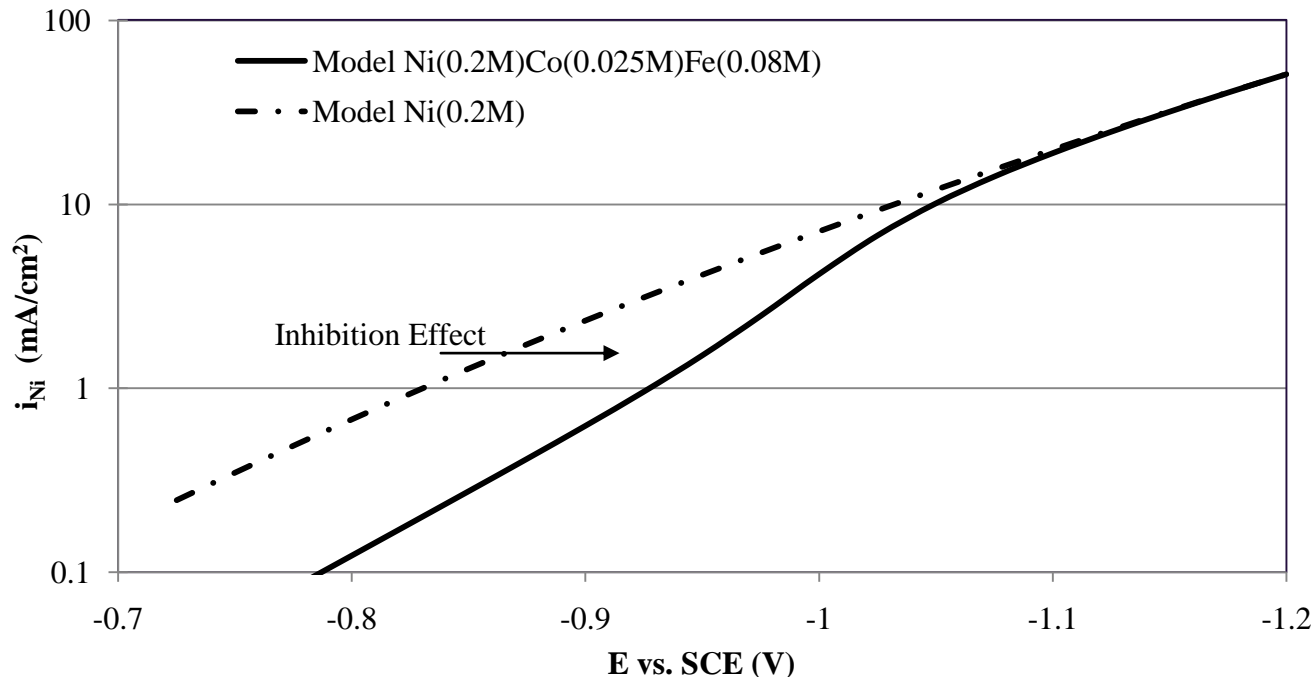


Figure 4-5: Inhibition effect simulation for nickel partial current density at a concentration of single metal deposition of 0.2M and ternary alloy deposition with changes in iron concentration of (a) alloy Fe(0.025M) (b) alloy Fe(0.08M) . (Fig. 4-5 continued)

(b)



Surface coverage simulation by iron species during ternary alloy deposition is shown in Figure 4-6. Most of the surface adsorption is found for FeNi^{+3} and FeCo^{+3} where Fe^+ is approximately zero and neglected during the simulation of alloy deposition. The same behavior is seen for cobalt, where the mixed metal rates are dominant. Nickel partial current density for alloys with different concentrations of iron is shown in Figure 4-7. Although it is not intuitive, the iron ions in the solution change the nickel rate. As the iron concentration is increased from 0.01M to 0.15M the nickel rate is reduced. The limiting value is reached at potentials more negative than -1.1V where the iron concentration no longer influences nickel's rate.

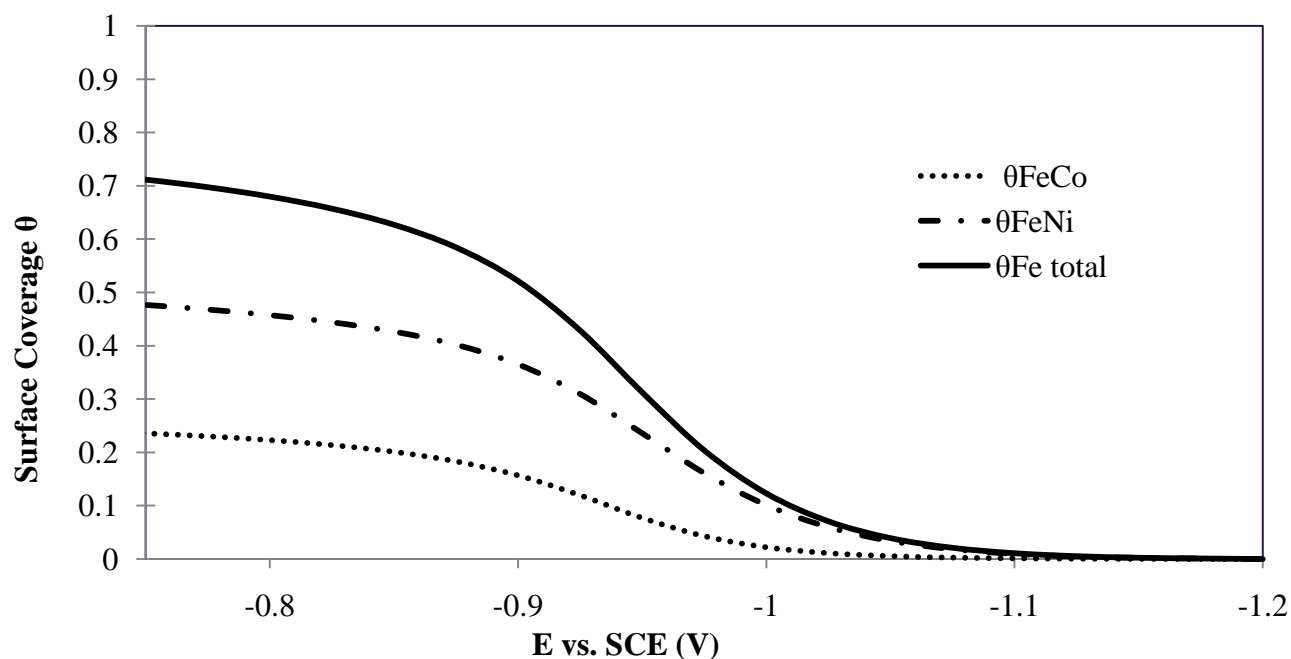


Figure 4-6: Surface coverage simulation by iron species during ternary alloy deposition of Ni(0.2M)Co(0.1M)Iron(0.025M).

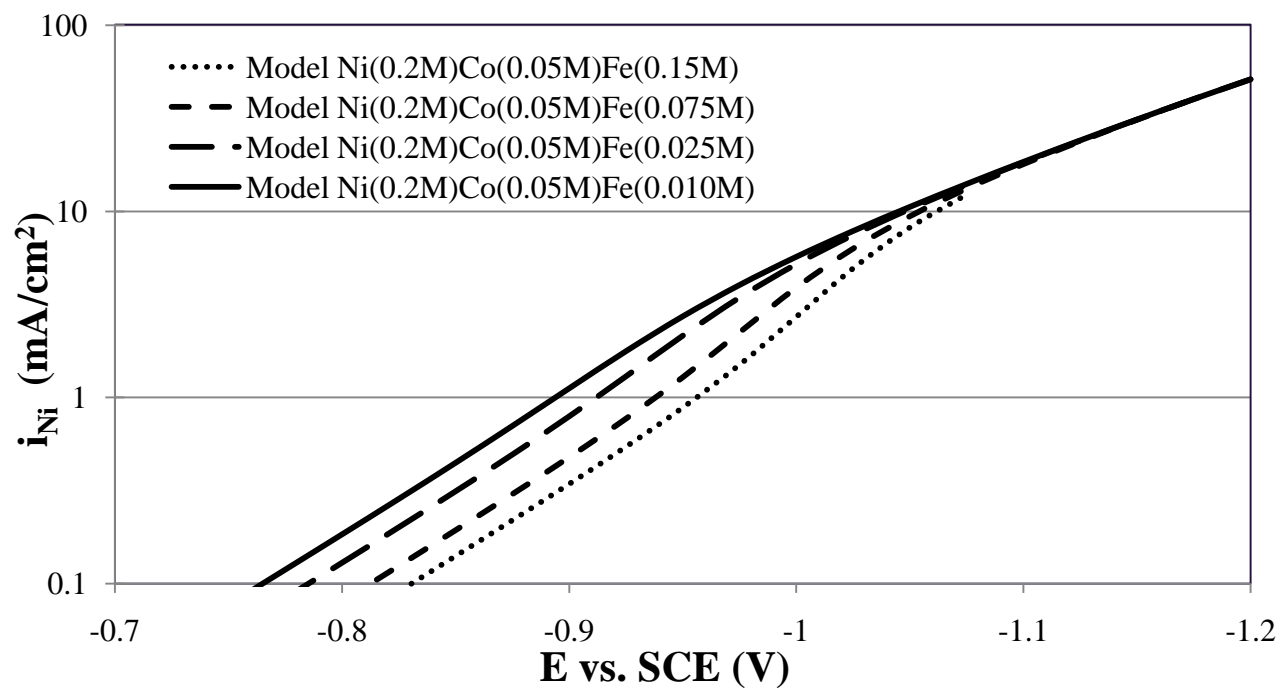


Figure 4-7: Influence of iron bulk concentration on the partial current density of nickel.

4.8 Confidence Regions and Statistical Results

Confidence intervals provide an indication of how far the estimate is expected from its true value⁴². Additionally, when two or more parameters are estimated in conjunction, confidence regions can be used to evaluate the correlation between parameters and their variation. This analysis and characterization steps are essential, especially when parameter uncertainty does exist and for model validation. Whenever possible and appropriate it is recommended that confidence regions be presented in addition to estimates. While confidence intervals are specified for individual parameters as an upper and lower limit, confidence regions are given as hyper-ellipsoids when errors are assumed additive, zero mean and, normal. In addition, the covariance matrix should be known⁴⁴.

$$(b - \beta)^T P^{-1} (b - \beta) = r^2 \quad [4.14]$$

Where $P = \sigma^2(X^T V^{-1} X)^{-1}$ and r^2 gives an idea of the confidence on the intervals. The hyper-ellipsoid defined as before is centered on the estimated values of the parameters. Results from estimated parameters for single metal deposition of Ni (0.2M) are used to show in Figure 4-8,4-9 and 4-10 the resulting 95% confidence ellipsoids and confidence intervals, for rate constants and inverse Tafel slopes. Figures 4.8 and 4.9 contain the y axis rate constant and x-axis the inverse Tafel slope, it can be seen that the high inclination of the ellipsoid indicates that in fact, there is a strong correlation between the rate constants and the inverse Tafel slope. Also the degree of the ellipsoid indicates that the uncertainty of the parameters is about the same. Figure 4-10 shows the confidence ellipsoid of both Tafel slopes where as expected there is less correlation and small uncertainty between the two inverse Tafel slopes.

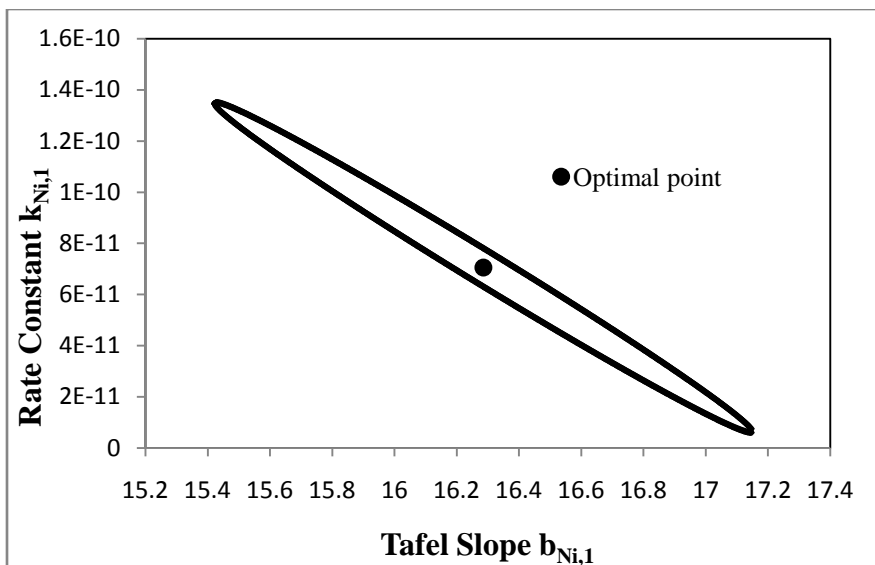


Figure 4-8: Confidence ellipsoid for Tafel slope and rate constant of Ni for reaction one.

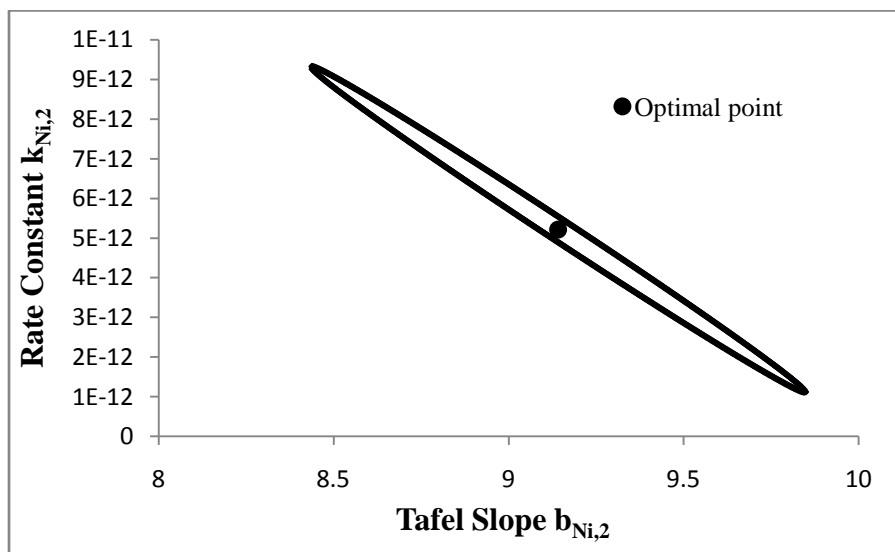


Figure 4-9: Confidence ellipsoid for Tafel slope and rate constant of Ni for reaction two.

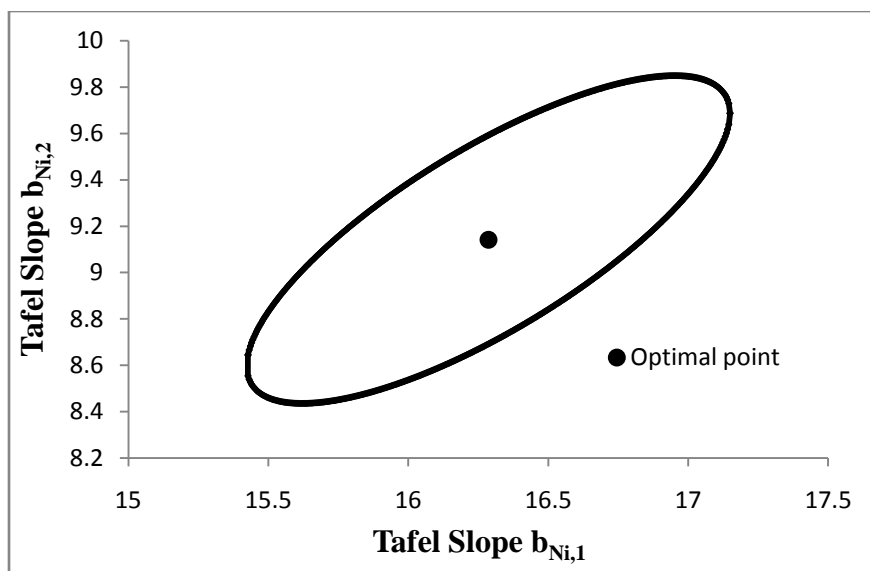


Figure 4-10: Confidence ellipsoid for Tafel slopes of Ni reactions.

Estimation of the parameters and the statistical analysis of the results depend strongly on the given standard deviations of the measurement errors as well as on the variance model and values of the respective variance model given. The statistical analysis also depends on the available experimental data provided. If the available experimental data is insufficient for the estimation the statistical analysis may show large confidence intervals for the associated parameters, even though the fit may be very good. The information about the nature of surface coverage is qualitative and no experimental data is available. From the point of view of the estimation problem, this can also contribute to the lack in the experimental information, although the users can qualitative input some ranges for these results. Some large confidence intervals were found for some estimation, mainly due to insufficient available data for the estimation. Another factor that contributed to unrealistic confidence ellipsoids is the various orders of magnitude difference between some parameters.

CHAPTER 5. OPTIMIZATION STUDIES

The electrochemical models developed and implemented in gPROMS are used to study mass transfer and reaction kinetics of alloy depositions. Parameter estimation techniques have succeeded in estimating kinetic parameters for a range of concentrations to create a generalized model. This generalized model can be used to test and study experimental procedures to develop interesting depositions with unique characteristics. Using optimization techniques the models can be used to optimize experimental operations to devise plans and procedures for improved operation of existing electrochemical systems procedures.

5.1 Introduction

Optimization theory is derived from a body of mathematical results and numerical methods, it refers to identify and find the best candidate from a collection of alternatives without having to explicitly enumerate and evaluate all possible alternatives. The root of engineering lies directly in the process of optimization where engineering design involves describing the process mathematically and selecting a solution to an engineering problem. Design of new and more efficient systems as well as to devise plans and manufacturing procedures for improved operations is a critical function of engineering practice⁴³. Optimization methods have been found from modest level mathematics for developing algorithms involved in iterative numerical calculations, using clearly defined logical procedures⁴⁴. Therefore the methodology requires a range of mathematical theories into vector-matrix manipulations, calculus, algebra and elements of real analysis. The success of optimization of engineering problems depends on:

- Defining the system boundaries.
- Selecting the performance criterion.
- Selection of independent variables.
- Formulation of the model.

System boundaries involve interactions and limits which are taken into consideration to approximate the real system. Performance criteria are selected to minimize or maximize the value of performance index. Independent variables are chosen to adequately characterize design and operating conditions of the system. After the performance criterion and independent variables have been identified the formulation of the system model is used which describes the basic material and energy balance equations for engineering systems⁴⁵.

In electrodeposition systems, interesting materials with a range of properties are deposited into a substrate by manipulating variables such as potential, current, concentrations and other key variables. Fabrication involves experimental testing, where advanced models could play a big role into further understanding behaviors of the systems as well as facilitating the study of key variables to deposit materials with important properties. By applying process optimization techniques into well structured models, engineers can achieve significant improvements in fabrication and quality of electrodeposition process.

5.2 Optimization Overview: Objective Function

A construction of a robust model is critical for optimization problems. The model needs to behave properly for the entire range of possible values of control variables and time invariant parameters. The optimization depends critically on the accuracy of the process models used in the computational scheme. Optimality is defined as the maximization or minimization of an objective function where additional equality and or inequality constraints are not violated. A set of unknowns or variables which affect the objective function are contained in the mathematical model, a selection of the independent variables it's important to include the ones that have most impact on the composite system. The process model by considering mixed differential and algebraic equations is specified as follows:

$$f(x(t), \dot{x}(t), y(t), u(t), v) = 0 \quad [5.1]$$

where x and y denote the differential and algebraic variables respectively, $\dot{x}(t)$ variable with time derivative, $u(t)$ the control variable and v a time invariant parameter to be determined during optimization. The differential and algebraic variables should be tested to remain within specified bounds for changes in values of u and v .

The objective function for optimization problem seeks to determine time horizons and values of the time invariant parameters v as well as time variation of control variables $u(t)$ over the entire time horizon, where the objective is to minimize or maximize the value of the objective function z , which can be either a differential variable x or a algebraic variable y . The performance criterion will either be the maximum or minimum value of any performance objective function chosen. The selection of the objective function can be one of the most important factors in the optimization design process, depending on the situation an obvious objective function may exist. The bounds on optimization decision variables where time horizon will be subject to lower and upper bounds also could be a fixed value. Control variables and time invariant parameters will be subject to lower and upper bounds. Mathematically the objective function takes the form:

$$\min_{v, u(t), t_f, t \in [0, t_f]} z(t_f) \quad [5.2]$$

$$u^{min} \leq u \leq u^{max} \quad [5.3]$$

$$v^{min} \leq v \leq v^{max} \quad [5.4]$$

$$t_f^{min} \leq t_f \leq t_f^{max} \quad [5.5]$$

Most optimization problems have a single objective function for scalar value although multi-objective optimization for vector values is also possible. When no objective function is used, then the goal is to find a set of variables that satisfies the constraint of the model, this

problem is called a feasibility problem. An extra algebraic equation is added to the model for several variables to be optimized

$$z = \emptyset(x, \dot{x}, y, u, v) \quad [5.6]$$

Design variables need to satisfy certain specified functions and cannot be chosen arbitrarily, these restrictions are called design constraints, that represent limitations. Constraints can be imposed in the optimization problem, such as³⁴:

End point constraint: $w(t_f) = w^*$ [5.7]

$$w^{min} \leq w(t_f) \leq w^{max} \quad [5.8]$$

Interior point constraint: $w_i^{min} \leq w(t_i) \leq w_i^{max}$ [5.9]

Path constraint: $w^{min} \leq w(t) \leq w^{max}$ [5.10]

5.2.1 Point and Dynamic Optimization in gPROMS

gPROMS optimization entity can optimize steady state or dynamic behavior of complex model systems. Both design and operational optimization can be carried out using the general form of the objective function and constraints. Decision variables can be time invariant or dependent on time. The mathematical description equation 5.1 although assumes that the system in terms of ordinary differential and algebraic equations can be applicable to time invariant systems for one or more space dimensions.

Consideration regarding specific control variables over time is specified during dynamic optimization³⁴. The different types are:

- Piecewise-constant controls
- Piecewise-linear controls
- Piecewise-linear continuous controls
- Polynomial controls

Steady state optimization problems are special cases of point optimization where time invariant controls are used. Same specifications are used as in dynamic mode where obviously time horizon section is omitted. The initial conditions of the system are specified as steady state.

Optimization results are generated in gPROMS files PPP which is the execution entity.

The four output files consist of:

- Comprehensive optimization report file (PPP): This contains quick access to general information such as objective function values and information on decision variables.
- Optimization report file (PPP.out): This contains a simple summary of the optimization execution:
 - outcome of run,
 - objective function final value,
 - time horizon and length of time intervals final value,
 - time invariant parameters and control variable profiles and
 - values for variables on which constraints are specified.
- Schedule file (PPP.Schedule): Provides contents of a gPROMS schedule that can be copied directly into a simulation. The detailed optimal results can be reproduced by a simulation activity.
- Point file (PPP.point): provides results at each iteration of the optimization, which results are the same as the schedule file. It is used to restart optimization after a failure, while being able to provide good initial guesses.

5.3 Practical Applications

There is a range of problems that can be solved using point and dynamic optimization which would be practically impossible without this entity. This section will use some examples

to show the power of the optimization entity and some applications to our model. Some general problems where optimization entity can be useful consist of the following:

- Some empirical work is available for alloys where deposits with various compositions result from varying the current and potentials. The bulk concentrations are usually fixed, and varied to find new results. All combinations of bulk concentrations of the electrolyte cannot be practically tested experimentally. An electrodeposition model that has been tested and validated against a range of concentrations can be used to optimize the desired compositions by not only varying the current or potential but the bulk concentrations as well. Point optimization can be used to tackle these types of problems as in example problem 1. Figure 5-1 shows an example where it would be impossible to obtain a composition consisting of 10% iron, 10% nickel and 80% cobalt alloy with a fixed concentration of the electrolyte of 0.2M nickel, 0.05M cobalt and 0.05M iron.
- Multilayer systems such as Huang's quaternary system have been tested empirically using a specified electrolyte concentration to deposit layers with certain thickness. It is important to control, the thickness of each layer as well as the current or potential needed to achieve each composition required using. A dynamic optimization problem such as problem 2 can be implemented to be able to schedule deposits with properties of interest.

Problem 1: A specified composition of 50% Iron, 50% Cobalt, and 0% Nickel is wanted from an electrolyte containing the metals of interest. What bulk concentrations of the metals are needed in the electrolyte, and what potential should the deposition take place at to reach our desired composition. Since our model is composed of a ternary NiCoFe system, nickel will be included in the problem and will be used as the objective function in order to minimize the composition to a value of zero. Table 5.1 contains the point optimization problem specified and results.

Problem 2: For the quaternary system, where a specified electrolyte is used to deposit multilayers, potential needs to be varied, in order to preferentially deposit each layers. Copper deposits at a lower potential than iron, nickel and cobalt. The proposed optimization will minimize the objective function, by controlling the total current. The constraint variables will consist of 100% composition of copper and the rest of the metals composition set to zero. It is also important to control the thickness of deposits which will depend on the time of the deposition as well as current densities of the metals shown in equation 2.24. The next multilayer will consist of a known alloy composition that is feasible with the concentration specified, where an optimization problem with the specified composition constraints will be performed. The inequality end point constraints consist of compositions of the alloy to be 65% cobalt, 20% copper, 10 % iron and 5 % nickel. The dynamic optimization will determine the thickness of the deposit for the alloy. The results should reveal a schedule for experiment consisting of the time and potentials that needs to be used for multilayer deposits. Tables 5.2a and 5.2b show the results.

5.3.1 Optimization Execution

The standard solver used for optimization consists of CVP_SS and CVP_MS which can solve optimization problems for mixed integer optimization, which constitutes both discrete and continuous decision variables. The solvers are based on control vector parameterization approach. The control vector assume a piecewise constant or linear functions of time over a number of intervals. Depending on the problem a single shooting or multiple shooting optimizations are used. For problem number 2 the dynamic optimization involves time invariant parameters which are specified by the optimizer. The solvers use a DASOLV code to find the solution of DAE problems and solve for sensitivities. The solver supports steady state and non steady state problems with continuous decision variables.

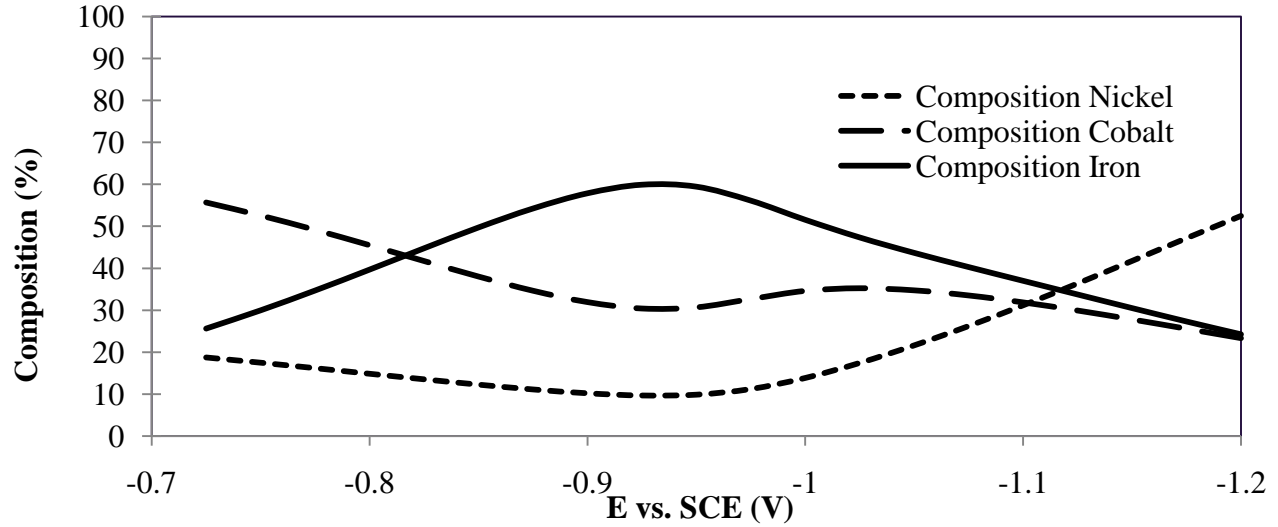


Figure 5-1: Example of a fixed concentration of electrolyte, composition vs. potential (V)

Table 5-1: Point optimization problem 1 results

Objective Function (minimize): Composition of Nickel			
Control Variables	Initial guess	lower bound	upper bound
$C_{Co\ bulk} [mol\ cm^{-3}]$	5.00E-05	2.50E-05	1.00E-04
$C_{Fe\ bulk} [mol\ cm^{-3}]$	5.00E-05	2.50E-05	1.00E-04
$C_{Ni\ bulk} [mol\ cm^{-3}]$	1.00E-06	0	2.00E-04
Potential [V]	-1	-1.2	-0.7
Inequality end point Constraints			
		lower bound	upper bound
Composition of Cobalt [%]		49	51
Composition of Iron [%]		49	51
Results from point optimization problem			
Objective function being minimized:	0		
$C_{Co\ bulk} [mol\ cm^{-3}]$	0.0001		
$C_{Fe\ bulk} [mol\ cm^{-3}]$	3.60E-05		
$C_{Ni\ bulk} [mol\ cm^{-3}]$	0		
Potential [V]	-1.02186		
Constrained Variable Type			
Composition of Cobalt [%]	49.6		
Composition of Iron [%]	50.39		

Table 5-2: Dynamic optimization problem 2 part a results

Objective Function (minimize) : Potential [V]

Control Variables	initial guess	lower bound	upper bound
Total Current [mA/cm ²]	3	0.01	5
Inequality end point Constraints		lower bound	upper bound
Composition Cobalt [%]		0	0.1
Composition of Copper [%]		99.5	100
Composition of Iron [%]		0	0.1
Composition of Nickel [%]		0	0.1
Thickness of the deposit [nm]		12	12.5

Results from dynamic optimization problem

Objective function being minimized: -0.2395

Time to obtain thickness of deposit : 100 s

Parameters

Total Current [mA/cm ²]	0.335
-------------------------------------	-------

Constrained Variable Type

Composition of Cobalt [%]	0
Composition of Copper [%]	100
Composition of Iron [%]	0
Composition of Nickel [%]	0
Thickness of the deposit [nm]	11.99

Table 5-3: Dynamic optimization problem 2 part b results

Objective Function (maximize) : Potential [V]			
Control Variables	initial guess	lower bound	upper bound
Total Current	32	25	41
Inequality end point Constraints		lower bound	upper bound
Composition of Cobalt [%]		73	74
Composition of Copper [%]		8	9
Composition of Iron [%]		14	15
Composition of Nickel [%]		3.5	4
Thickness of the deposit [nm]		193	195
 Results from dynamic optimization problem			
Objective function being minimized:	-1.023		
Time to obtain thickness of deposit :	83.26		
Parameters			
Total Current [mA/cm ²]	33.06		
Constrained Variable Type			
Composition of Cobalt [%]	73		
Composition of Copper [%]	8.87		
Composition of Iron [%]	14.16		
Composition of Nickel [%]	2.96		
Thickness of the deposit [nm]	194.76		

The optimization results as shown in table 1 for a specified composition of 50% cobalt and iron are achieved with a 0.3 deviation. The bulk concentrations of the electrolyte consist of iron 0.36M and cobalt 0.1M. The potential is set to -1.02V. All results are on the range of lower and upper bounds specified. By taking the advantage of point optimization entity in the electrodeposition alloy systems a range of compositions of the alloys is possible by varying the

concentrations of the electrolyte and potential or current. The second problem dynamic simulation is executed to control compositions of layers as well as time required for thickness of each layer. For a copper layer a potential of -0.2395 V at 100 seconds of the deposition is found to deposit 100% copper with a thickness of 11.99 nm. The next layer results indicate a need to change the potential to -1.023 for 83.26 seconds to be able to deposit an alloy composition of 73% cobalt, 8.9% copper, 14.1% iron and 3% nickel with a thickness of 194.76. Dynamic optimization is successful in its execution. A schedule report file from gPROMS containing the time and potentials to be applied are given, where the code can be directly imputed into the process model for gPROMS simulation. The schedule sequence to reproduce multilayer deposition for the specified system is given. Table 5-4 shows the schedule sequence which results are graphed in figure 5.4

Table 5-4: gPROMS schedule sequence for the process entity

```
SEQUENCE
  RESET
    THE.ITOT := 0.335;
  END
  CONTINUE FOR 100
  RESET
    THE.ITOT := 33.06;
  END
  CONTINUE FOR 83.26
END
```

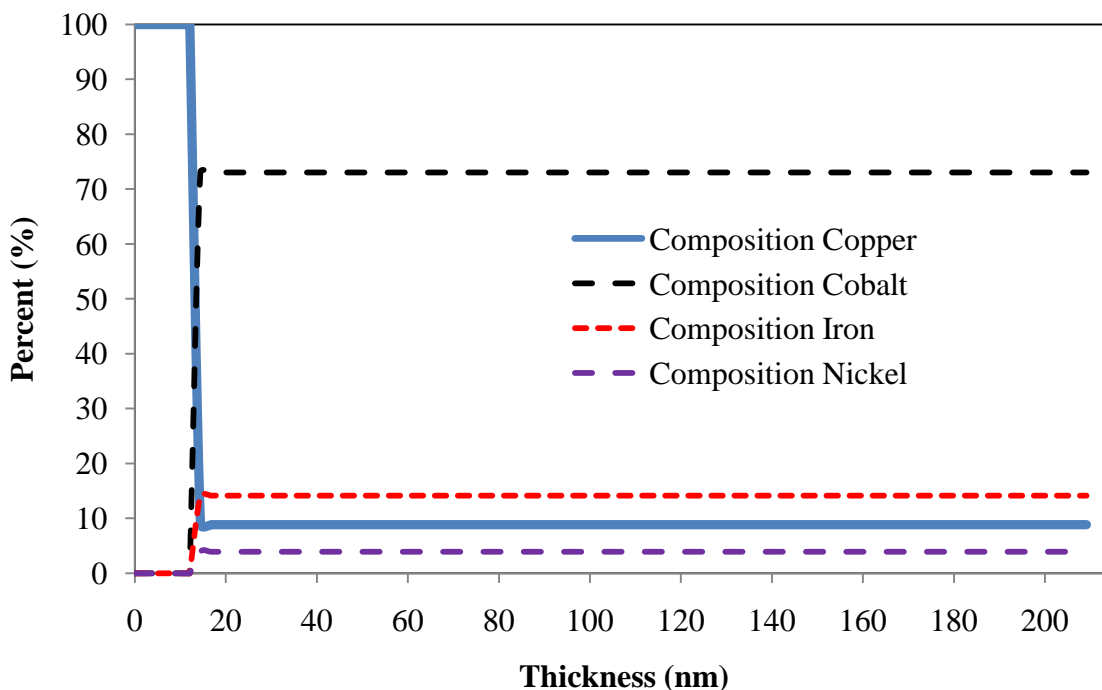


Figure 5-2: Metal compositions vs. thickness (nm)

5.4 Optimization Studies Conclusion

In this chapter dynamic and point optimization has been introduced to the electrodeposition complex model. The detailed mechanistic model for steady state NiCoFe and dynamic NiCoFeCu/Cu includes diffusion equations relating concentrations to time and distance from the electrode surface. The second order parabolic partial differential equations concentration dynamics contain transport equations and chemical reactions. Due to the complex nature the system, the control vector parameterization approach from gPROMS solvers is used. Constraints to account for other objectives of the process are included in the execution. Not only is the point optimization objective functions resolved for determining optimal bulk concentrations of electrolyte and potentials but sequence schedule are also developed for multilayer depositions. At this level, experimental validations should be carried to fine tune the process model variables and equations for further optimizing the electrodeposition system model.

CHAPTER 6. CONCLUSIONS

Formulation and Implementation of the models to characterize the electrodeposition of ternary NiCoFe and quaternary NiCoFeCu/Cu deposition into gPROMS advanced modeling language was successfully performed. An introduction into the implementation of the solvers used was found where the scale of the complex system is critical when assigning tolerance for convergence. Variables initial values are also critical for initialization of the simulations solvers. Parameter estimation techniques were tested and implemented to estimate key kinetic parameters to cover for a whole range of operating conditions. Optimizations problems were defined and tested successfully using a single model to investigate novel deposition schemes. A front end application was built using the capabilities of modern open simulation architectures into excel and VBA. The main results and conclusions are listed as follows:

1. Using the mathematical model equations from both models, the implementation on an advanced modeling software was successful. Key specifications need to be given to solvers because of the scales associated with the equations. Most specifically in the case of convergence tolerance for the differential equations where to distinguish between concentrations of and rate constants of different orders of magnitude absolute tolerance was specified as low as $1e-9$ which proved to handle simulations well.
2. The most critical objective was to find a set of parameters for the whole range of concentrations which was not successful with previous version of trial and error estimates. A Maximum likelihood estimator was implemented and tested successfully for estimating single metal deposition rate constants and inverse Tafel slopes as well as for mixed metal intermediate kinetic constants. Table 4.2 and 4.3 show a single set of kinetic parameters for the range of concentrations used for estimating. The results are tested and validated against experimental

data. The same technique can be implemented into future electrodeposition systems with a larger number of metals, which increases the reactions and number of parameters to be estimated.

3. By taking advantage of the general model developed and the capabilities of modern simulation architectures a model centric environment was developed. The proposed environment can be fully used to study deposition behavior as well as investigation of novel fabrication schemes. A user friendly front end application is created in Excel with VBA using go:Run license to run the simulation directly from excel with gPROMS running at the background. The implementation is successful, and the application can be expanded to more complex systems easily. With this application non programming users can evaluate characteristics of the model and can be easily transferred to non expert users.

4. Optimization algorithms with clearly defined logical procedure were successfully investigated to solve non-trivial problems using point and dynamic optimization. A clearly defined problem for point optimization was solved to find the potentials and bulk concentrations of the electrolyte needed to get a fixed composition of 50% nickel and 50% cobalt. A dynamic optimization problem was also defined to obtain a scheduled sequence for depositing multilayers of NiCoFeCu/Cu where time of deposition dictates a defined thickness of the deposit as well potential controls which layer is deposited. It is clear that these two examples are just samples of a number of possible interesting problems that can be formulated using the proposed model-centric framework.

The following are some recommendations for future work:

- Availability of more experimental data for a larger range of concentrations will allow to fine tune currently estimated parameters more precisely and more importantly to be able to characterize completely the uncertainty (confidence) intervals.

- The model can be expanded to more metal depositions with additional reactions, to be used for further studies.
- Optimization results should be compared to experimental data to validate them, and be able to validate the model into fabricating materials of interest, by manipulating the composition as well as thickness of deposits.

REFERENCES

1. Zhuang Y, Podlaha EJ. NiCoFe Ternary Alloy Deposition: I. An Experimental Kinetic Study *Journal of the Electrochemical Society*. 2000; 147:2231.
2. Zhuang Y, Podlaha EJ. NiCoFe Ternary Alloy Deposition. *Journal of the Electrochemical Society*. 2003; 150:C219.
3. Zhuang Y, Podlaha EJ. NiCoFe Ternary Alloy Deposition. *Journal of the Electrochemical Society*. 2003; 150:C225.
4. Prutton M. *Thin Ferromagnetic Films*. Washington: Butterworths; 1964.
5. Mathias JA, Feddle GA. *IEEE Transactions on Magnetics*. 1969; 5: 728.
6. Mukasa K, Sato M, Maeda M. *Journal of the Electrochemical Society*. 1970; 117: 22.
7. Venkatesetty HV. *Journal of the Electrochemical Society*. 1970; 117:403.
8. Romankiw LT, Croll IM, Hatzakis M. *IEEE Transactions on Magnetics*. 1970; 6:597.
9. Ross CA. *Annu. Rev. Mater. Sci*. 1994; 24:159.
10. Sun L, Hao Y, Chien CL et al. *IBM J. Res. & Dev*. 2005; 49:79.
11. Baibich MN, Broto JM, Fert A et al. *Physical Review Letters*. 1998; 61: 2472.
12. Jimbo M, Kanda T, Goto S, Tsunashima S, Uchiyama S. *Journal of Magnetism and Magnetic Materials*. 1993; 126:422.
13. Matlosz M. Competitive Adsorption Effects in the Electrodeposition of Iron-Nickel Alloys. *Journal of the Electrochemical Society*. 1993; 140:2272.
14. Hessami S, Tobias CW. A Mathematical Model for Anomalous Codeposition of Nickel-Iron on a Rotating Disk Electrode. *Journal of the Electrochemical Society*. 1989; 136: 4611.
15. Sasaki KY, Talbot JB. Electrodeposition of Binary Iron-Group Alloys. *Journal of the Electrochemical Society*. 1995; 142:775.
16. Sasaki KY, Talbot JB. Electrodeposition of Iron-Group Metals and Binary Alloys from Sulfate Baths. *Journal of the Electrochemical Society*. 1998; 145:981.
17. Huang Q, Podlaha EJ. Electrodeposition of FeCoNiCu/Cu Compositionally Modulated Multilayers. *Journal of the Electrochemical Society*. 2002; 149:C349.
18. Huang Q, Podlaha EJ. Simulation of Pulsed Electrodeposition for Giant Magnetoresistance FeCoNiCu/Cu Multilayers. *Journal of the Electrochemical Society*. 2004; 151:C119.

19. Brenner A. Electrodeposition of Alloys. *Academic Press*. 1962; I:77.
20. Zech N, Podlaha E.J, Landolt D. *Journal of Applied Electrochemistry*, 1998; 11:1251-1260.
21. Sorenson HW, *Parameter Estimation: Principles and Problems*. New York: Marcel Dekker; 1980.
22. Englezos P, Kalogerakis N. *Applied Parameter Estimation for Chemical Engineers*. New York: Marcel Dekker; 2001.
23. Rolandi PA, Romagnoli JA. An integrated environment for support of process operations, *AIChE Annual Meeting*. 2005.
24. Rolandi PA, Romagnoli, JA. Integrated model-centric framework for support of manufacturing operations. Part i: The framework. *Computers and Chemical Engineering*, Submitted for publication. 2006a.
25. Rolandi PA, Romagnoli JA. Integrated model-centric framework for support of manufacturing operations. Part iii: Joint parameter estimation and data reconciliation. *Computers and Chemical Engineering*, Submitted for publication. 2006b.
26. Dini JW. *The Materials Science of Coatings and Substrates*. New Jersey: Noyes Publications; 1993.
27. Osaka, T. *Electrochimica Acta*, 2000; 45:3311.
28. Osaka T, Tadoka M, Hayashi K, et al. *Nature*. 1998; 392:796.
29. Cooper EI, Bonhôte C, Heidmann JY, et al. *IBM J. Res. & Dev.* 2005; 49:103.
30. Andricacos PC, Robertson N. *IBM Journal of Research and Development*. 1998; 42-5:671.
31. Phan NH, Schwarz M, Nobe K. *Plating and Surface Finishing*. 1998; 75.
32. Phan NH, Schwartz M, Nobe K. *Journal of Applied Electrochemistry*. 1991; 21: 672.
33. Huang Q. *Electrodeposition of FeCoNiCu Quaternary System*. Louisiana State University: Dissertation; 2004.
34. Zhuang Y. *Mechanism of the NiCoFe Ternary Alloy Deposition*. Louisiana State University: Dissertation; 2002.
35. Eisenberg M, Tobais CW, Wilke CR, *Journal of the Electrochemical Society*. 1954;101:306.
36. Levich VG, *Physicochemical Hydrodynamics*, New York: Prentice Hall; 1962.
37. Alden J. *Computational Electrochemistry*. Oxford University: Thesis; 1998.

38. Foss BA, Lohmann B, Marquardt W. A field study of the industrial modeling process. *Journal of Process Control*. 1998; 8:325-338.
39. Process Systems Enterprise Ltd. *gPROMS Introductory User Guide*, Release 2.3.1, United Kingdom: 2004.
40. Process Systems Enterprise Ltd. *gPROMS Advanced User Guide*, Release 2.3, United Kingdom: 2004.
41. Nagelkerke, NJD. Maximum Likelihood Estimation of Functional Relationships. *Lecture Notes in Statistics*. 1992; 69:13.
42. Beck JV, Arnold KJ. *Parameter Estimation in Engineering and Science*. New York: Wiley; 1977.
43. Fox RL. *Optimization Methods for Engineering Design*. Philippines: Addison-Wesley; 1971.
44. Ray WH, Szekely J. *Process Optimization*. Canada: John Wiley & Sons; 1973.
45. Reklaitis GV, Ravindran A, Ragsdell KM. *Engineering Optimization Methods and Applications*. Canada: John Wiley & Sons; 1983.

VITA

Miguel E. Estrada was born April 1984, to Eduardo J. Estrada and Kati L. Rijana, in Caracas, Venezuela. He completed his high school education in Tulsa, Oklahoma. He was accepted by University of Tulsa into the chemical engineering program and earned a Bachelor of Science degree May 2005. He was then awarded an assistantship to pursue a Master of Science degree in the Department of Chemical Engineering at Louisiana State University. He has started to work as a project engineer since August 2007, at Occidental Oil and Gas Corporation and hopes to develop and pursue his career in the petroleum industry.